

Editorial Manager(tm) for International Journal of Geomechanics
Manuscript Draft

Manuscript Number: GMENG-85R1

Title: Numerical prediction of the dynamic behaviour of two earth dams in Italy using a fully-coupled non-linear approach

Article Type: Technical Paper

Corresponding Author: Dr. GAETANO ELIA, Ph.D.

Corresponding Author's Institution: Newcastle University

First Author: GAETANO ELIA, Ph.D.

Order of Authors: GAETANO ELIA, Ph.D.; ANGELO AMOROSI, Ph.D.; ANDREW H.C. CHAN, Ph.D.;
MICHAEL J. KAVVADAS, Ph.D.

Abstract: The paper deals with the seismic stability assessment of two existing earth dams in Italy using a fully-coupled effective stress non-linear approach implemented in a finite element (FE) code. The mechanical behaviour of the involved clayey and granular soils is described through advanced elasto-plastic constitutive models, calibrated on laboratory and in-situ test results. Before the application of the seismic motions, appropriate FE static analyses are performed in both cases to define the initial stress state and the internal variables of the material models. The stability of both dams during dynamic loading is proved by the inspection of the cumulated horizontal and vertical displacement time histories of the monitored solid nodes, which become constant immediately after the end of the seismic actions. Moreover, the computed crest settlements induced by the earthquakes are considerably lower than the service freeboard of the dams. Being the applied seismic actions characterized by high return periods, the presented results are indicative of a satisfactory dynamic performance of the two embankments during extreme dynamic loading conditions.

Suggested Reviewers: Vaughan GRIFFITHS Ph.D.

Professor, Division of Engineering, Colorado School of Mines, Colorado, USA
d.v.griffiths@mines.edu

Prof. Griffiths has been particularly interested in the numerical prediction of the dynamic response of artificial and natural slopes since long time. His contribution to this class of problems has been valuable and precious (e.g. Woodward and Griffiths, 1996).

Opposed Reviewers:

Newcastle upon Tyne, 13 June 2010

To the Editor of the International Journal of Geomechanics

Dear Editor,

in response to the request of minor revisions to the paper No. GMENG-85 “Numerical prediction of the dynamic behaviour of two earth dams in Italy using a fully-coupled non-linear approach” by Gaetano Elia, Angelo Amorosi, Andrew H. C. Chan and Michael J. Kavvadas, I submit to your kind attention the revised manuscript and a detailed response to the reviewers' criticisms.

The paper is presented for the Special Issue on “Material and Computer Modeling”, guest edited by Chandra S. Desai, M. M. Zaman and D. N. Singh.

For any problem, please do not hesitate to contact me.

Many thanks in advance.

Best regards,

Gaetano Elia

Corresponding author:

Dr. Gaetano Elia

Lecturer in Geotechnical Engineering

School of Civil Engineering and Geosciences

Newcastle University

NE1 7RU Newcastle upon Tyne, United Kingdom

Tel: 0044 (0)191 2227934

E-mail: gaetano.elia@ncl.ac.uk

Title:

Numerical prediction of the dynamic behaviour of two earth dams in Italy using a fully-coupled non-linear approach

Authors:

Gaetano Elia¹, Angelo Amorosi², Andrew H. C. Chan³, Michael J. Kavvadas⁴

¹ Lecturer, School of Civil Engineering and Geosciences, Newcastle University, Drummond Building, NE1 7RU Newcastle upon Tyne, United Kingdom - formerly, Technical University of Bari, Italy (corresponding author). E-mail: gaetano.elia@ncl.ac.uk

² Associate Professor, Dept. of ~~Water Engineering and Chemistry~~~~Civil and Environmental Engineering~~, Technical University of Bari, via Orabona 4, 70125 Bari, Italy. E-mail: a.amorosi@poliba.it

³ Professor, School of Civil Engineering, The University of Birmingham, Edgbaston, B15 2TT Birmingham, United Kingdom. E-mail: a.h.chan@bham.ac.uk

⁴ Associate Professor, Dept. of Geotechnical Engineering, National Technical University of Athens, Iroon Polytechniou 9, Zografou 157 80, Athens, Greece. E-mail: kavvadas@central.ntua.gr

Abstract

The paper deals with the seismic stability assessment of two existing earth dams in Italy using a fully-coupled effective stress non-linear approach implemented in a finite element (FE) code. The mechanical behaviour of the involved clayey and granular soils is described through advanced elasto-plastic constitutive models, calibrated on laboratory and in-situ test results. Before the application of the seismic motions, appropriate FE static analyses are performed in both cases to define the initial stress state and the internal variables of the material models.

The stability of both dams during dynamic loading is proved by the inspection of the cumulated horizontal and vertical displacement time histories of the monitored solid nodes, which become constant immediately after the end of the seismic actions. Moreover, the computed crest settlements induced by the earthquakes are considerably lower than the service freeboard of the dams. Being the applied seismic actions characterised by high return periods, the presented results are indicative of a satisfactory dynamic performance of the two embankments during extreme dynamic loading conditions.

CE Database subject headings:

Embankment stability; Earthquake loads; Constitutive models; Finite element method; Soil dynamics.

1. Introduction

The construction sites of a number of earth dams and embankments, built all over the world, were once considered as non-seismic in the past. Recent evolution of the seismic hazard mapping requires a careful assessment or re-assessment of the dynamic stability of a significant number of such existing structures. In fact, consistent with modern performance-based approaches, the analysis of the effects of seismic loads on the stability and serviceability conditions becomes crucial to establish and manage the safe operation of such existing earth dams in the future.

The dynamic response of earth embankments has been usually analysed using pseudo-static analyses, displacement methods derived from Newmark (1965)'s rigid block model or by means of site response analyses based on the equivalent visco-elastic method (e.g. Schnabel *et al.*, 1972), extended linear approaches (e.g. Kausel and Assimaki, 2002; Delépine *et al.*, 2009) or more advanced hypotheses (e.g. Borja *et al.*, 1999; Bonilla *et al.*, 2005; Amorosi *et al.*, 2010).

To perform advanced FE dynamic analyses of this class of geotechnical structures, the fully-coupled effective stress formulation for the solid-fluid interaction (Biot, 1941; Zienkiewicz *et al.*, 1999) has received increasing attention in recent years (e.g. Arulanandan and Scott, 1993; Dewoolkar *et al.*, 2001; Dakoulas and Gazetas, 2005, 2008; Liu and Song, 2005). At the same time, it is relevant to describe with appropriate constitutive models the essential features of the mechanical behaviour of soils when subjected to cyclic loading, such as state dependency, early irreversibly, non-linearity, build up of excess pore water pressures, evolution of microstructure (de-structuring) and related decrease of nominal stiffness (e.g. Sangrey *et al.*, 1969; Castro and Christian, 1976; Vucetic and Dobry, 1991). In this respect, a number of advanced models have been proposed within the framework of Critical State Soil Mechanics, all developed by adding further features to the classical single surface Modified Cam-Clay model, in order to capture the soil

1 response under both monotonic and cyclic loading conditions (e.g. Dafalias and Popov, 1975; Mroz
2 *et al.*, 1978; Prevost, 1978; Bardet, 1986). The implementation of these non-linear constitutive
3
4 models into numerical codes has, therefore, significantly improved the prediction capabilities of the
5
6 stress-strain response of large dams during static service conditions and under seismic loading (e.g.
7
8 Elgamal *et al.*, 2002; Aydingun and Adalier, 2003; Muraleetharan *et al.*, 2004; Amorosi *et al.*,
9
10 2008; Sica *et al.*, 2008).
11
12
13
14
15

16
17 In this paper the dynamic behaviour of two existing earth dams located in the south of Italy, one
18
19 homogeneous and one zoned, is studied using a fully-coupled non-linear approach. The constitutive
20
21 assumptions for the clayey materials of the embankments and the foundation deposits and the
22
23 granular soils of the shells are the Model for Structured Soils (*MSS*), proposed by Kavvadas and
24
25 Amorosi (2000), and the Pastor-Zienkiewicz Mark III model (*PZ3*) developed by Pastor *et al.*
26
27 (1990), respectively.
28
29
30

31 The same procedure is adopted to study the dynamic behaviour of the two dams: after a brief
32
33 description of the geometrical and geotechnical characteristics of the two structures, a discussion of
34
35 the constitutive models calibration, based on laboratory and in-situ tests results, is presented.
36
37
38

39 In order to define the initial stress state and the corresponding values of the internal variables in the
40
41 material models, appropriate FE static analyses are performed to simulate a simplified geological
42
43 history of the deposit, the dam construction stages and the reservoir impounding before the
44
45 application of the input seismic signals at the bedrock level. Finally, a class A prediction of the
46
47 dynamic response of the dams under different seismic motions is illustrated in terms of signal
48
49 amplification, permanent excess pore water pressures and cumulated displacements during the
50
51 seismic loading. The behaviour of the embankments is also analysed during the consolidation stage
52
53
54
55
56 at the end of the earthquake action.
57
58
59
60
61
62
63
64
65

2. The Finite Element code and the constitutive models adopted

The non commercial program used in this work is *DIANA-SWANDYNE II* (Dynamic Interaction And Non-linear Analysis-SWANsea DYNamic program version II), a two-dimensional (plane strain and axi-symmetric) FE code that implements the fully-coupled Biot (1941) dynamic equations using the u - p simplification (where u is the skeleton displacement and p the pore pressure), i.e. assuming that the fluid acceleration relative to the solid skeleton is negligible. The code can be used for static, consolidation, and dynamic analyses carried out under drained and undrained conditions. The mathematical and numerical formulation of the code is described in detail by Chan (1995) and Zienkiewicz *et al.* (1999). The employed time integration scheme is the GNpj method (Generalised Newmark p th order scheme for j th order equation) proposed by Katona and Zienkiewicz (1985). In the solution of the Biot dynamic equations the code allows to introduce the viscous damping to account for non-plasticity related damping and to supplement the amount of hysteretic damping required by the geotechnical system under study. Viscous damping is included via the frequency dependent Rayleigh damping matrix (Clough and Penzien, 1993).

The constitutive model adopted for the cohesive soils involved in the numerical simulations presented in the paper is the Model for Structured Soils (*MSS*) developed by Kavvadas and Amorosi (2000) for structured clayey materials. The model, based on multi-surface plasticity concepts, is characterised by two nested Cam-Clay like elliptical surfaces in the stress space: the external one, called Bond Strength Envelope (BSE), which represents the material states associated with the onset of degradation of structure at appreciable rate, and the internal yield surface (PYE) geometrically similar to the BSE, but scaled by a factor $\xi \ll 1$. For states inside the PYE, the behaviour is reversible and described by stress dependent bulk and shear moduli. For the states on the PYE, early irreversibility is accounted for by the onset of plastic strain. In this case, when the PYE and BSE surfaces are not in contact, the model predicts a realistic degradation of the soil stiffness, controlled

1 by the smooth decay of the hardening modulus with the distance between the surfaces. Once the
2 two surfaces are in contact, the formulation coincides with that of a single surface Modified Cam-
3 Clay like model. *MSS* includes both isotropic and kinematic hardening. The isotropic hardening rule
4 controls the size of the BSE, i.e. it describes the evolution of material bonding by means of a
5 damage-type mechanism to model volumetric and deviatoric structure degradation, whereas the
6 kinematic hardening rules describe the motion of the two characteristic surfaces in the stress space
7 and thus account for the evolution of material anisotropy. The formulation of *MSS* allows the model
8 to reproduce some of the key features of the cyclic behaviour of clays as the decay of the shear
9 stiffness with strain amplitude, the corresponding increase of hysteretic damping and the related
10 accumulation of excess pore water pressure under undrained conditions (Amorosi and Kavvadas,
11 1999; Elia, 2004; Elia *et al.*, 2004).

12 The stress-strain behaviour of the granular soils involved in the presented finite element analyses
13 has been simulated through the Pastor-Zienkiewicz Mark III model (*PZ3*), developed within the
14 framework of generalized plasticity. The failure condition is based on the Critical State Theory,
15 which postulates that all residual states lie on a unique line in $p'-q-e$ space (where p' , q and e
16 are the mean effective stress, the deviatoric stress and the soil void ratio, respectively), regardless of
17 the stress path followed. However, deviatoric hardening is also included so that the critical state line
18 (or sometimes called phase transformation line) can be crossed for the first time when modelling
19 undrained behaviour of dense sand before returning to it at failure. Consistently with experimental
20 evidence for cohesionless soils, the model uses a non-associative flow rule for modelling the
21 behaviour within the hardening region. The *PZ3* model does not require the explicit definition of the
22 yield and potential functions, but only of the direction vectors normal to each surface. The direction
23 of the plastic strain increment vector depends on dilatancy, which is approximated by a linear
24 function of the stress ratio $\eta = q / p'$. In contrast to classical plasticity, the model does not require
25 the application of the consistency condition to define the hardening modulus. This considerably

simplifies the computational aspects and improves computational efficiency. As the elastic modulus and loading hardening modulus are all scaled by the mean effective stress, the soil model achieves very low values for the elastic and plastic moduli when liquefaction occurs and this is consistent with physical observations. For loose contractive sand *PZ3* predicts the densification and strain-hardening in drained shear and the development of excess pore pressure and liquefaction in undrained shear. For very dense dilative sands in drained shear the model accounts for strain-softening and residual conditions at the critical state. Comparisons between predictions of the original model and experimental data on undrained monotonic loading of contractive and dilative sands, on cyclic loading leading to liquefaction of very loose sands and on cyclic mobility of dense sands showed very good agreement (Pastor *et al.*, 1990). Detailed descriptions of the basic model are given in the original publications by Pastor and Zienkiewicz (1986) and Pastor *et al.* (1990).

3. The Marana Capacciotti dam

The first embankment studied in the present work is the homogeneous earth dam located in Puglia, south-east of Italy, along the Marana Capacciotti stream, about 13.5km south-west of the city of Cerignola (FG, Italy). The embankment was built between 1970 and 1975 using cohesive materials (represented mainly by sandy and clayey silts of low plasticity) with homogeneous granulometry and index properties (Calabresi *et al.*, 2000). It has a volume of $3.71 \times 10^6 \text{ m}^3$ and retains $49 \times 10^6 \text{ m}^3$ of water with a service freeboard of 2.6m. With respect to its main cross-section (Figure 1), the dam is 48m high and has a base of 370.5m; it overlays a foundation soil composed by a first layer of a slightly overconsolidated alluvial silt, with a thickness of about 12m, and a deeper stiff overconsolidated silty clay deposit. The drainage system consists of a sub-vertical drain, that discharges the water into a tunnel parallel to the dam longitudinal axis, and of a drain disposed at the toe of the downstream slope. An impervious concrete diaphragm located in the alluvial silt layer along the centre line of the dam prevents the seepage flow underneath the embankment.

1 The seismic behaviour of the Marana Capacciotti dam has been already described by Elia *et al.*
2 (2010). In this paper the constitutive model calibration and the static analyses results are briefly
3
4 illustrated, while a more detailed discussion on the effects of different boundary conditions on the
5
6 FE dynamic results is presented. The additional settlements of the embankment due to the
7
8 dissipation of the excess pore pressures cumulated during the earthquake action are also evaluated.
9
10

11 12 13 14 *3.1 Constitutive model calibration* 15

16
17 In the case of the Marana Capacciotti dam, the *MSS* model has been used to simulate the
18
19 mechanical behaviour of both the natural clayey soil deposit and the cohesive material of the
20
21 embankment. In order to re-assess the dynamic stability of the dam, a new geotechnical
22
23 characterization of the site was recently carried out (Calabresi *et al.*, 2000): in particular, 21
24
25 undisturbed samples, obtained from three boreholes performed along the dam crest (named S1 and
26
27 S2 in Figure 1) and the downstream slope (S3), were tested in the laboratory and the main
28
29 experimental results have been used to calibrate the constitutive model adopted in the static and
30
31 dynamic numerical simulations. Specifically, the results of oedometer and undrained triaxial
32
33 compression (CU-TRX) tests have been used to calibrate the *MSS* model for static loading
34
35 conditions, while the results of resonant column (RC) and bender element (BE) tests have been
36
37 employed to assess the small-strain shear stiffness profile along the dam axis and to calibrate the
38
39 model parameters for cyclic/dynamic loads.
40
41
42
43
44
45

46 A detailed description of the model calibration procedure for the different soils involved in the FE
47
48 analyses of the dam is reported in Elia *et al.* (2010) and is not discussed here.
49
50
51
52

53 *3.2 Finite element model of the dam and static analysis results* 54 55

56 The numerical analyses of the Marana Capacciotti dam have been performed using the mesh shown
57
58 in Figure 2. In order to minimise the lateral boundary effects during the dynamic analyses, the
59
60 length of the foundation layer has been chosen to be three times the base of the dam. Moreover, on
61
62
63
64
65

the left and right side of the foundation layer, viscous boundaries have been simulated using two columns of finite elements characterised by a Rayleigh damping equal to 25%, in order to avoid wave reflections along the boundaries of the mesh during the seismic action. These far-field boundary conditions have been already employed in the past (Elia *et al.*, 2005; Amorosi *et al.*, 2008) and their efficiency has been recently analysed by Semblat *et al.* (2010). A discussion on the effectiveness of those absorbing boundaries ~~The correctness of these choices is proved~~ presented in the following ~~final part of the paper~~ section.

No direct seismic site measurements were available to characterise the shear stiffness profile with depth of the deep silty clay stratum. Therefore, the thickness of the bedrock formation to be assumed in the FE discretization has been selected based on typical shear wave velocity profiles obtained by in-situ tests performed in similar sites located in the same region and characterised by comparable geotechnical conditions (Mucciarelli and Gallipoli, 2006). As a result, a shear wave velocity of 800m/s (typical of a bedrock formation) was reached within the first 30m of the stiff clay layer and, consequently, a foundation soil deposit of 42m (12m of alluvial soil and 30m of stiff clay) has been considered in both static and dynamic numerical simulations. A mesh of 794 isoparametric quadrilateral finite elements with 8 solid nodes and 4 fluid nodes has been used, assuming plane strain free draining condition for all the analyses. The solid nodes at the bottom of the mesh have been fixed in both the vertical and horizontal directions, while the nodes on the lateral sides of the mesh have been fixed in the horizontal direction only.

As discussed in the previous section, the mechanical behaviour of both the natural clayey soil foundation layers and the embankment cohesive soil has been modelled using *MSS*. The internal variables of this constitutive model, i.e. the position and dimension of the two characteristic surfaces in the stress space, allow to keep track of the material anisotropy, non-linearity and irreversibility. Therefore, their initial values play a significant role in the simulated dynamic behaviour of the dam and, as such, should be initialised consistently with the previously experienced stress history of the soil. This implies that, in order to obtain realistic results from the

dynamic analyses, appropriate FE static simulations have been performed before the application of the seismic action at the bedrock level in order to reproduce a simplified, though realistic, geological history of the deposit, the following dam construction and the subsequent reservoir impounding stages (Elia *et al.*, 2010). Once the static analyses of the dam and its foundation layer have been completed, the stress states and the values of the internal variables of the constitutive model have been checked to be consistent with the laboratory data. For this purpose, Figure 3 illustrates the profile of the initial shear modulus G_0 with mean effective stress predicted along the dam axis by the assumed constitutive model at the end of the static analyses: the computed values of the small-strain shear modulus are in fair agreement with the experimental ones, also reported in the figure.

3.3 Dynamic analysis results

The stability assessment of real earth dams subjected to dynamic loading requires the definition of the input ground motion at the bedrock level based on a site specific seismic hazard study.

For the evaluation of the dynamic stability of the Marana Capacciotti dam the results of a seismic hazard study carried out by the Italian National Institute of Geophysics and Volcanology (INGV) on the entire Italian territory have been used (Gruppo di lavoro MPS, 2004). From the INGV interactive maps of seismic hazard (<http://esse1-gis.mi.ingv.it/>), a peak ground acceleration of 0.275g can be obtained at the dam site for a return period of 1000 years and 0.194g for a return period of 475 years. Three acceleration time histories have been selected from a database of earthquake records (Ambraseys *et al.*, 2000) and linearly scaled to the mentioned maximum acceleration values. Appropriate techniques should be fulfilled to select real records, scale and match them to target spectra (e.g. Hancock *et al.*, 2008), but this is beyond the purpose of the paper.

The peak ground accelerations predicted by the seismic hazard study are referred to input motions recorded at the ground surface, i.e. at the “outcropping” rock. In the dynamic analyses of the dam, the scaled records have been filtered to a maximum frequency of 10Hz, transferred to the “inside”

1 bedrock formation through a standard de-convolution analysis and applied at the base of the FE
2 discretization of the system (as suggested by Kwok *et al.*, 2007). The relevant characteristics of the
3
4 obtained input motions are listed in Table I in terms of return period (T_R) at the dam site, maximum
5
6
7 acceleration (a_{max}), maximum frequency content (f_{max}), dominant frequency and record length. The
8
9
10 corresponding acceleration time histories are shown in Figure 4.

11
12 The dynamic behaviour of the Marana Capacciotti dam has been studied with the code *DIANA-*
13
14 *SWANDYNE II* by applying the above mentioned real input motions to the ~~fixed~~-solid nodes at the
15
16 base of the mesh (now fixed in the vertical direction only) as prescribed horizontal displacement
17
18
19 time histories.

20
21 Differently from what presented in Elia *et al.* (2010), the results of the fully-coupled FE dynamic
22
23 analysis of the dam subjected to the E-W horizontal component of the accelerogram registered at
24
25 Nocera Umbra (PG, Italy) during the earthquake of September 1997 (characterised by a moment
26
27 magnitude $M_w = 6.0$ and a surface-wave magnitude $M_s = 5.9$) are discussed here in detail. The
28
29 applied seismic motion (indicated as *NOCERA* in Table I) has a peak ground acceleration of 0.148g,
30
31
32 a length of 40s and a dominant frequency of 2.63Hz. Its Fourier spectrum is plotted with a thick
33
34
35 black solid line in Figure 5(a). The dynamic response of the dam has been studied for a duration of
36
37
38 60s, using a time step of 0.01s, equal to the time interval of the earthquake trace.

39
40 A Generalized Newmark time-stepping procedure has been used for time integration during the
41
42 dynamic simulation, with algorithm parameters equal to $\beta_1 = 0.6$ and $\beta_2 = 0.605$ for the solid
43
44 phase and $\beta_1^* = 0.6$ for the fluid phase, in order to obtain an unconditionally stable time-step
45
46
47 scheme (Zienkiewicz *et al.*, 1999). The small numerical damping introduced by these values has
48
49
50 been proved not to be sufficient to remove spurious high frequencies due to the finite element
51
52
53 ~~discretization~~discretisation. As the hysteretic damping provided by the adopted constitutive model
54
55
56 is very small for cycles with a shear strain amplitude smaller than 0.001% (Elia *et al.*, 2010), the
57
58
59 addition of a small amount of viscous damping of the Rayleigh type has been necessary in the FE
60
61
62
63
64
65

dynamic analysis of the dam. At this scope, a user-defined elastic stiffness matrix has been employed for the Rayleigh damping matrix calculation, assuming different constant values of the stiffness parameters with depth consistently with the stress state predicted at the same depth at the end of the static analyses. After a preliminary parametric study of the problem, a damping ratio equal to 2%, associated to the frequencies of 0.477Hz-48Hz and 2.385Hz, has proved to be effective in reducing the unrealistic amplification of the high frequencies during the seismic excitation of the dam (Elia *et al.*, 2010) and has been adopted in all the FE dynamic simulations of the dam.

Figure 5(a) shows the comparison between the input motion applied at the bedrock and the acceleration time histories computed along the dam axis at the crest of the embankment and at the dam base in terms of Fourier spectra. The results indicate that the amplification of the seismic signal ~~occurs~~occurs between the bedrock and the crest: the peak ground acceleration at the top of the dam is equal to 0.39g, with a magnification factor of about 2.6 over the peak bedrock amplitude. The energy content of the seismic wave computed at the crest level is concentrated in the range 0 to 6Hz, with the highest amplification effect at 0.85Hz and a maximum peak of the spectral acceleration at 2.69Hz, corresponding to the dominant frequency of the bedrock signal. Furthermore, the adopted viscous damping manages to restrict the high frequencies amplification effect of the input motion, which nevertheless still occurs during the simulation.

As mentioned before, the far-field boundaries have been simulated using two columns of elements (30m wide), disposed along the left and right side of the dam foundation layer (Figure 2) and characterised by a Rayleigh damping equal to 25%. In order to prove the effectiveness of this choice, the dynamic analysis of the dam has been re-run assuming different boundary conditions: in a first case, the two columns of elements with 25% of Rayleigh damping have been removed (this simulation has been named “no viscous boundaries”). Repeatable boundary conditions (Zienkiewicz *et al.*, 1999) have been applied at the vertical sides of the foundation layer in a second FE simulation, named “tied-nodes”. Moreover, the free-field response has been obtained applying the

NOCERA input motion at the base of a soil column (42m high and 5m wide) representative of the foundation layer only (without the dam), using the tied-nodes boundary conditions. The material states and the MSS internal variables obtained at the end of the static analyses of the dam along a vertical far from both the mesh boundaries and the dam axis ($x = 555.5$ m, Figure 2) have been used as input for this third dynamic simulation. The results of this latter analysis (named “1D response”), representative of the free-field response of the foundation layer, have been compared with the ones obtained during the previously presented FE simulation (named “viscous boundaries”) and during the other two additional dynamic analyses performed without viscous boundaries and employing the tied-nodes boundaries, respectively. The comparison, presented in terms of Fourier spectra of the acceleration time histories recorded at ground level along the vertical at $x = 555.5$ m, is shown in Figure 5(b). The dynamic behaviour of the foundation layer obtained during the three 2D simulations is similar, regardless of the adopted boundary conditions, and results in good agreement with the free-field response, thus indicating that the adopted length of the mesh is sufficient to avoid wave reflections along the vertical boundaries during the seismic action. The same resemblance between the three 2D dynamic analyses results has been observed along different monitored verticals throughout the mesh, thus indicating that the adopted boundary conditions have a negligible effect on the results of the presented FE dynamic simulation.

~~The evolution with time of the vertical and horizontal displacements (relative to the bedrock) of the nodes displaced along the dam axis is~~The contour lines of horizontal and vertical displacements obtained at the end of the dynamic simulation are shown in Figures 6(a) and 6(b), respectively. In these figures and the following ones, the horizontal displacements are positive when the movement is from left to right while the vertical displacements are negative when directed downwards. The advanced constitutive assumption adopted in the FE analysis allows the realistic simulation of the non-linear and irreversible response of the soils subjected to the dynamic action, leading to a final permanent horizontal displacement of the crest equal to 0.35m and a crest settlement of 0.54m, essentially due to plastic strains accumulation throughout the shaking. The computed displacement

time histories become constant immediately after the end of the earthquake (i.e. after 40 s) in all the monitored nodes, indicating a stable behaviour of the dam once the seismic action is over.

The overall behaviour of the dam in terms of displacement points out a greater deformation pattern of the downstream slope with respect to the upstream one, but does not give a precise indication of the occurrence of a failure mechanism inside the embankment and its foundation layer. Being the seismic action applied at the bedrock very demanding ($T_R = 1000$ years), the results can be considered indicative of a satisfactory dynamic performance of the dam in this extreme condition.

As the FE code *DIANA-SWANDYNE II* is based on an effective stress formulation, it allows the user to monitor the pore pressure regime at every single node of the mesh during the simulations. The contour lines of excess pore water pressures computed at the end of the earthquake are plotted in

Figure 7: i) the accumulation of negative pore pressures during the shaking is observed in the portions of the embankment close to the surface, as the cohesive soil in this part of the dam is highly overconsolidated due to the static compaction; ii) the central part of the embankment, the alluvial silt layer and the silty clay soil below the dam are characterized by positive excess pore pressures because the material state at the end of the static analysis is slightly overconsolidated; iii) in the remaining part of the silty clay deposit negative pore pressures cumulate as the initial state of the material has not been affected by the weight of the embankment and still lies on the side dry of critical.

Although it was not directly imposed by the user, the system behaves in undrained conditions during and after the shaking, the materials permeabilities being too low to allow the dissipation in 60s of the excess pore water pressures cumulated during the first 40s. At the end of the dynamic simulation, the satisfaction of the equilibrium condition for both the solid and the fluid phase has been imposed (i.e. a long term, fully drained, condition has also been considered). This leads to further settlements of the downstream slope of about 0.025m. The contour lines of the vertical displacements induced by the excess pore pressures dissipation are shown in Figure 8.

1
2 Finally, the contour lines of the shear strains (in absolute value) cumulated after 40s are reported in
3
4 Figure 9, showing the seismic induced concentration of plastic strains propagating from the toe of
5
6 the downstream slope into the alluvial silt layer.
7
8
9

10 11 **4. The San Pietro dam** 12 13

14
15 The San Pietro dam is located in Campania, southern Italy, along the Osento stream, between the
16
17 towns of Aquilonia (AV, Italy) and Monteverde (AV, Italy).
18
19

20 The embankment has a volume of $2.2 \times 10^6 \text{ m}^3$ and retains $17.7 \times 10^6 \text{ m}^3$ of water with a
21
22 freeboard of 2.0m at the maximum impounding level of the reservoir. It was built in the early 60's,
23
24 using clayey silts of low plasticity for the core and granular soils for the shells. With reference to its
25
26 main cross-section (Figure 10), the dam is 49m high and has a base of 250m; it overlays a
27
28 foundation soil composed by a first layer of alluvial gravels, with an average thickness of 7m, and a
29
30 deeper stiff overconsolidated flysch deposit. Two sub-vertical drains are interposed between the
31
32 clayey core and the shells. During the construction, the alluvial layer mechanical properties were
33
34 improved by concrete injections, also reducing the soil permeability. Moreover, the seepage flow
35
36 underneath the embankment is prevented by an impervious concrete diaphragm, disposed along the
37
38 centre line of the dam and reaching the flysch deposit.
39
40
41
42
43

44 The same procedure employed for the stability analysis of the Marana Capacciotti dam has been
45
46 adopted to study the dynamic response of the San Pietro dam, as described in the following: at first,
47
48 the advanced constitutive models used to simulate the mechanical behaviour of the clayey and
49
50 granular soils of the embankment have been calibrated against laboratory and in-situ data, then
51
52 appropriate FE static analyses have been performed to initialize the material states and the model
53
54 internal variables and, finally, the seismic action has been applied at the bedrock level to evaluate
55
56 the dynamic response of the dam.
57
58
59
60
61
62
63
64
65

4.1 Constitutive models calibration

Also in the case of the San Pietro dam, the re-assessment of its dynamic stability has required an improved geotechnical characterization of the embankment site (Calabresi *et al.*, 2004): 31 undisturbed samples, obtained from five boreholes performed along the dam crest (named S1 in Figure 10), the downstream slope (S2 and S3) and outside the dam on the downstream side (S4 and S5), were tested in the laboratory. Moreover, five cross-hole (CH) tests were performed close to the boreholes, while two CPT and three SCPT tests were performed along the dam crest and the downstream slope.

~~ESpecifically,~~ for the core material the results of oedometer and undrained triaxial compression tests have been used to calibrate the *MSS* model for static loading conditions, while cross-hole, resonant column and bender element tests have been employed to assess the small-strain shear stiffness profile along the dam axis and to calibrate the model parameters for cyclic and dynamic loads. The *PZ3* model has been calibrated with reference to the in-situ test results relative to the gravel used for the dam shells and standard literature curves (Vucetic and Dobry, 1991) relating the decay of shear modulus with cyclic shear strain to the material plasticity index.

As regards the core silty clay soil, the results of the undrained triaxial compression tests carried out on sample S1-C6 (borehole S1, depth 18m) at different consolidation pressures are reported in Figure 11 (solid line) as stress paths in the $p'-q$ plane, deviatoric stress - axial strain ($q - \varepsilon_a$) and pore pressure - axial strain ($u - \varepsilon_a$) curves. Dashed lines in the same figure show the corresponding *MSS* predictions: a part from the positive deviatoric hardening shown during the test performed at the highest consolidation pressure, the model simulations are able to catch the fundamental features of the material mechanical behaviour. For the same soil, Figure 12 shows the experimental results obtained from two different RC tests carried out on sample S1-C5 (borehole S1, depth 15m) in terms of normalised shear modulus G/G_0 with cyclic shear strain γ . The corresponding prediction

of the *MSS* model, reported in the same figure with a dashed line, is in reasonable agreement with the laboratory data.

A more detailed description of the models calibration for the soils involved in the FE analyses of the San Pietro dam is reported in Rampello *et al.* (2005) and is not discussed here.

4.2 Finite element model of the dam and static analysis results

The mesh adopted for the numerical analyses of the San Pietro dam is shown in Figure 13. The CH measurements indicate that the bedrock formation can be identified at a depth of 25m below the base of the embankment: therefore, a foundation soil deposit composed of 7m of alluvial gravels and 18m of flysch has been considered in the static numerical simulations. A mesh of 894 isoparametric quadrilateral finite elements with 4 solid and 4 fluid nodes has been used, assuming plane strain and free draining condition for all the analyses. The same boundary conditions adopted for the Marana Capacciotti dam along the bottom and the vertical sides of the mesh have been here employed. The sub-vertical drains have been simulated using the same constitutive model adopted for the core of the dam but imposing a permeability value intermediate between those assumed for the core and the shells of the embankment. A linear elastic model has been employed to simulate the mechanical behaviour of both the alluvial layer treated with concrete injections, the stiff overconsolidated flysch deposit and the impervious concrete diaphragm using the appropriate elastic properties and permeability values coming from in-situ measurements.

After the simulation of the geological history of the deposit and the dam construction and compaction phase layer by layer, the impounding stage has been analysed imposing a reservoir level 4.5m below the crest. The pore water pressure distribution obtained at the end of the seepage analysis is reported in Figure 14: the maximum value of suction attained in the upper part of the dam is equal to 20kPa at the crest.

At the end of the static analyses, the profiles of the initial shear modulus G_0 with the mean effective stress predicted by the employed constitutive models have been compared with the laboratory and

in-situ data: for the core clayey soil, the computed values of the small-strain shear modulus represent a reasonable compromise between the experimental values obtained by the BE tests and the ones observed during the cross-hole measurements (CH1), which are usually higher (Figure 15(a)). In the case of the shells granular material (Figure 15(b)), for which no BE tests were available, the G_0 computed values are close to the lower bound of the CH measurements (CH2 and CH3).

Figure 16 shows the settlement profiles (Poulos *et al.*, 1972) computed along two verticals through the dam core (Figure 16(a)) and the downstream slope (Figure 16(b)) at the end of the static analyses: the obtained settlements at different depths are in good agreement with the values measured during the embankment construction (also reported in the same figure with solid lines and named A5, A7, A9 and A10), thus validating the calibration of the two constitutive models.

4.3 Dynamic analysis results

The dynamic behaviour of the San Pietro dam has been studied applying two different input motions directly at the base of the embankment, i.e. neglecting the wave propagation in the dam foundation layer due to the high stiffness of both the injected alluvial gravels and the overconsolidated flysch deposit. The first seismic motion is represented by the E-W horizontal component of the accelerogram registered at Bisaccia (AV, Italy) during the earthquake of November 1980, while the second is an artificially generated earthquake (Calabresi *et al.*, 2004).

For the dam site, the CNR-GNDT (Galadini *et al.*, ~~1999~~2000) seismic hazard study predicts a peak ground acceleration of 0.35g for a return period of 475 years. Therefore, the maximum acceleration of the real input motion and the elastic response spectrum, from which the artificial earthquake has been generated, have been scaled to this reference value. The main characteristics of the two input ground motions are summarized in Table II in terms of return period (T_R), maximum acceleration (a_{max}) and velocity (v_{max}), bracketed duration (T_D), Arias intensity (I_A), maximum frequency

content (f_{max}), dominant frequency and record length. The artificial earthquake has a frequency content compatible with the design spectrum proposed by Eurocode 8 for a soil of type A and is not characterised by a well-defined dominant period. On the contrary, the real input action has a frequency content limited in the range 0.5÷1.1Hz and is characterised by a much higher energy content with respect to the artificially generated accelerogram. The FE dynamic simulation performed using the real accelerogram has a time length of 80s, while the seismic response of the embankment subjected to the artificial earthquake has been studied for a duration of 40s, using a time step of 0.01s in both cases.

A small amount of Rayleigh damping, (equal to 3%) for the frequencies 1.27Hz and 3.90Hz, has been added in the FE dynamic simulations, while the numerical damping introduced by the time-stepping procedure has been reduced (with respect to the previously commented dynamic analysis of the Marana Capacciotti dam), employing algorithm parameters equal to $\beta_1 = 0.51$ and $\beta_2 = 0.515$ for the solid phase and $\beta_1^* = 0.51$ for the fluid phase.

Figure 17 shows the comparison in terms of Fourier spectra between the input motions applied at the base and the corresponding acceleration time histories computed, during the two simulations, along the dam axis at the crest of the embankment. The results point out the amplification of the seismic signal occurred in both cases between the base and the crest. The Fourier spectrum of the acceleration time history recorded at crest using the real input motion shows two peaks at 0.51Hz and 1.11Hz, corresponding to the dominant frequencies of the base signal, and the maximum peak at 2.6Hz59Hz, representing the first natural frequency of the system (Figure 17(a)). The same value of the dam fundamental frequency appears to be excited by the artificial earthquake: from Figure 17(b) it is evidentclear that the highest amplification effect of the input signal occurs again at 2.6Hz59Hz.

The results of the fully-coupled dynamic simulations are summarized in Figure 18 in terms of profiles with non-dimensional depth z/H of the ratio a_{max}/a_{base} between the maximum

1 acceleration recorded along the dam axis and the base input value. In both the analyses, the profiles
2 are characterised by a significant amplification of the seismic signal at the crest of the dam. In the
3
4 case of the real input motion, the peak acceleration at crest is equal to 0.93g, while applying the
5
6 artificial earthquake the corresponding maximum acceleration is equal to 0.81g, with a
7
8 magnification factor of about 2.3 over the peak base amplitude in both cases. Moreover, the results
9
10 are consistent with those obtained from the response analyses of different dams reported in the
11
12 literature (Cascone and Rampello, 2003) whose envelope is indicated in the same figure with the
13
14 shaded area.
15
16

17
18 The contour lines of horizontal and vertical displacements obtained at the end of the real earthquake
19
20 simulation are shown in Figures 19(a) and 19(b), respectively. The maximum crest settlement
21
22 relative to the dam base induced by the earthquake (equal to 0.68m) is equivalent to the 15% of the
23
24 service freeboard (4.5m) and to the 34% of the freeboard at the maximum impounding level of the
25
26 reservoir (2.0m). Similar results have been obtained in terms of final permanent horizontal and
27
28 vertical displacements when the artificial input motion is applied at the base (Figure 20): in this
29
30 case, the crest horizontal displacement is equal to 0.35m, while the maximum crest settlement is
31
32 equal to 0.77m, equivalent to the 17% of the service freeboard and to the 38.5% of the freeboard at
33
34 the highest impounding level.
35
36

37
38 More generally, the dam behaviour is stable during and after the dynamic input motions and no
39
40 failure mechanism inside the embankment can be recognized in both the FE simulations. As the
41
42 seismic actions applied at the base of the dam are very demanding (representing two “near field”
43
44 earthquakes), the overall results can be considered indicative of a satisfactory dynamic performance
45
46 of the embankment in these extreme conditions.
47
48

49
50 The evolution with time of the excess pore water pressures computed during the two FE dynamic
51
52 analyses in two fluid nodes (both placed in the dam core, along its axis, at a depth of 19 and 34m
53
54 from the crest, respectively) is reported in Figure 21: in both cases, positive excess pore pressures
55
56 cumulate at $z = 34$ m, with a maximum value of 250kPa when the real accelerogram is applied at
57
58
59
60
61
62
63
64
65

the base. On the contrary, the excess pore water pressures generated by the two earthquakes at $z = 19$ m are negative, reaching a peak value of about -300kPa during the real input motion analysis. This result is related to the initially strongly overconsolidated state of the core material at 19m depth from the crest, as a consequence of the simulation strategy employed to numerically reproduce the compaction procedure adopted in the construction of the core.

In any case, the cumulated pore water pressures tend to dissipate after the end of the seismic actions. This latter consolidation process, once simulated numerically, leads to negligible additional vertical displacements of the downstream slope and dam core, as indicated in Figure 22.

5. Comparison between the seismic response of the two dams

In the previous sections the seismic response of two real earth dams has been studied using similar procedures and approaches but applying different earthquakes at bedrock. In order to perform a direct comparison between the dynamic behaviour of the two embankments, the San Pietro dam has been subjected to the same *NOCERA* input motion used for the study of the Marana Capacciotti dam. The numerical damping introduced in this new simulation and the adopted Rayleigh parameters are the same of those employed for the Marana Capacciotti analysis. The results of this comparison are presented in Figure 23 in terms of Fourier spectra obtained at the crest of the two embankments: i) in both cases the signal is amplified at about 2.6Hz, close to the dominant frequency of the input motion (2.63Hz); ii) the Marana Capacciotti dam amplifies more the frequencies in the range 0.85÷1.56Hz, which are close to its fundamental period of vibration (equal to 1.21Hz, as shown by Elia *et al.* 2010), than those in the range 4.5÷5.5Hz; iii) in the San Pietro dam analysis some amplification occurs at 1.53Hz, but a larger amplification can be observed for the frequencies between 4.85 and 6.95Hz. Moreover, the figure shows a higher overall amplification effect in the case of the San Pietro dam, as the *NOCERA* earthquake is shaking the system close to its first natural period (2.59Hz). The same effect can be observed if the profiles of

a_{max} / a_{base} obtained along the two dam axes are compared (Figure 24(a)): a bigger amplification of the input signal occurs in the top part of the San Pietro dam, with an acceleration magnification factor at its crest of about 4.0 over the peak bedrock amplitude. The result is essentially correlated to a lower shear strain level induced by the seismic action in the San Pietro embankment, as indicated by Figure 24(b) where the profiles of maximum shear strain recorded along the two dam axes are reported with non-dimensional depth. The lower shear strain amplitude induced by the earthquake is accompanied by higher material stiffness and lower hysteretic damping during the shaking, thus enhancing the transmission of the high frequencies of the seismic signal and increasing the amplification of the peak acceleration at the surface. Nevertheless, the seismic induced displacements recorded during the San Pietro analysis are significantly lower than those induced by the same earthquake on the Marana Capacciotti dam, as shown in Figure 24(c) in terms of profiles of maximum horizontal displacement relative to the dam base recorded at the end of the simulations along the dam axes. According to the hazard studies, the first structure is in fact located in a seismic-prone zone characterised by higher peak ground accelerations for the same return periods with respect to the Marana Capacciotti embankment and, therefore, has been correctly designed and constructed with a higher initial shear stiffness in order to suffer lower structural deformations.

6. Conclusions

The seismic response of both the Marana Capacciotti and the San Pietro dam has been studied using a fully-coupled finite element code in which the mechanical behaviour of the involved materials has been simulated adopting advanced constitutive models. This kind of approach requires, especially during dynamic simulations, the choice of different quantities, such as the values of the parameters controlling the time-stepping scheme adopted in the code, the amount of viscous damping

introduced in the numerical analysis and the type of viscous boundaries used along the mesh sides, that can significantly control the results (e.g. Woodward and Griffiths, 1996).

As regards the boundary conditions, in the case of the Marana Capacciotti dam the far-field boundaries have been simulated using two columns of elements (30 m wide), disposed along the left and right side of the dam foundation layer (Figure 2), characterised by a Rayleigh damping equal to 25%. In order to prove the effectiveness of this choice, the dynamic analysis of the dam has been re-run, assuming different boundary conditions: in a first case, the two columns of elements with 25% of Rayleigh damping have been removed (this simulation has been named “no viscous boundaries”). Although the studied 2D geometry does not have a vertical axis of symmetry, the tied-nodes boundaries (Zienkiewicz *et al.*, 1999) have been applied at the vertical sides of the foundation layer in a second FE simulation, named “tied nodes”. Moreover, the free-field response has been obtained applying the *NOCERA* input motion at the base of a soil column (42 m high and 5 m wide) representative of the foundation layer only (without the dam), using the tied-nodes boundary conditions. The material states and the *MSS* internal variables obtained at the end of the static analyses of the dam along a vertical far from both the mesh boundaries and the dam axis ($x = 555.5$ m, Figure 2) have been used as input for this third dynamic simulation. The results of this latter analysis (named “1D response”), representative of the free-field response of the foundation layer, have been compared with the ones obtained during the previously presented FE simulation (named “viscous boundaries”) and during the other two additional dynamic analyses performed without viscous boundaries and employing the tied-nodes boundaries, respectively. The comparison, presented in terms of Fourier spectra of the acceleration time histories recorded at ground level along the vertical at $x = 555.5$ m, is shown in Figure 22. The dynamic behaviour of the foundation layer obtained during the three 2D simulations is similar, regardless of the adopted boundary conditions, and results in good agreement with the free-field response, thus indicating that the adopted length of the mesh is sufficient to avoid wave reflections along the vertical boundaries during the seismic action. The same resemblance between the three 2D dynamic analyses results

has been observed along different monitored verticals throughout the mesh, thus indicating that the adopted boundary conditions have a negligible effect on the results of the presented FE dynamic simulation.

Particular attention has also been given in this work to the influence of the viscous damping, fictitiously added during the FE dynamic simulations, on the numerical seismic behaviour of the dams. As the Rayleigh damping depends on the excitation frequency, the real amount of viscous damping involved in the dynamic analyses cannot be known *a priori*. A check on the amount of viscous damping acting in the analyses has been performed monitoring the energy dissipation that characterise the low amplitude residual oscillations of the system in the post-seismic stage of the simulations. In particular, following the approach usually adopted in structural dynamics to study the response of under critically damped single degree of freedom systems (Clough and Penzien, 1993), the effective damping ratio involved in the numerical simulations has been evaluated considering the reduction in amplitude of successive positive peaks of the horizontal time history recorded at the crest of the dams.

Figure 23 shows a detail of the previously presented evolution of the horizontal displacement of the Marana Capacciotti dam crest (see Figure 5(b)) in the range 40 to 60 s after the beginning of the shaking. The dam and its foundation layer oscillate around a final neutral position with a mean frequency of 1.21 Hz that can be considered the first natural frequency of the system. The average number of cycles required to give a 50% reduction in amplitude is equal to 8. The effective damping ratio calculated from different successive peaks of the considered displacement time history is equal to 1.55%: being the cycle amplitude very small, the computed damping ratio does not include the hysteretic damping provided by the MSS model and is representative of the real amount of viscous damping involved in the simulation at the natural frequency of the system. This value is close to the one used to calibrate the Rayleigh coefficients (i.e. 2% associated to the two frequencies 0.477 Hz and 2.385 Hz, corresponding to a damping ratio equal to 1.68% associated to

1.21 Hz), thus proving an *a posteriori* verification of the correctness of the Rayleigh damping calibration procedure adopted in this work.

The paper has highlighted the possible benefits deriving from the use of a fully-coupled effective stress non-linear approach in the analysis of the dynamic response of large earth embankments: the advanced constitutive models and the soil skeleton-pore fluid dynamic interaction scheme adopted in the simulations have allowed to reasonably estimate the permanent displacements of the dams and the development of excess pore water pressures inside the structures during the seismic action, providing a realistic prediction of the additional settlements due to consolidation. As no direct displacement and pore pressure measurements during real seismic motions are available, the results of the presented FE simulations represent a class A prediction of the dynamic response of the two embankments in view of modern performance-based design approaches.

In both cases, the stability of the dams has been proved by the inspection of the cumulated horizontal and vertical displacement time histories of the monitored solid nodes, which become constant immediately after the end of the seismic actions. Moreover, the computed crest settlements induced by the earthquakes resulted considerably lower than the threshold values imposed by the service freeboard of the dams. Being the applied seismic actions characterised by high return periods, the overall results can be considered indicative of a satisfactory dynamic performance of the two embankments during extreme seismic loading conditions.

Finally, the comparison between the dynamic response of the two dams, performed applying the same input motion at bedrock level, has shown how the propagation of the seismic wave inside the embankments and the corresponding dynamically induced deformations are significantly influenced by the combination between the energy content of the input signal, its relation to the natural frequencies of the structures and the mechanical properties of the involved soils in terms of initial shear stiffness and hysteretic damping.

Acknowledgements

The research was financially supported by the Italian Ministry of University and Scientific Research (PRIN-MIUR 2007/09). The Authors would like to thank Prof. S. Rampello and Dr. L. Callisto for allowing the use of some unpublished data. The help of the *Consorzio per la Bonifica della Capitanata*, currently managing the Marana Capacciotti and the San Pietro dam, is also acknowledged.

References

1. Ambraseys N., Smit P., Berardi R., Rinaldis D., Cotton F. and Berge C. (2000). Dissemination of European Strong-Motion Data (CD-ROM collection). European Commission, DGXII, Science, Research and Development, Bruxelles.
2. Amorosi A. and Kavvas M. (1999). A plasticity-based constitutive model for natural soils: a hierarchical approach. In: D. Kolymbas (Ed.), Proc. III Euroconference on Constitutive Modelling of Granular Materials, Horton, Greece, 413-438.
3. Amorosi A., Elia G., Chan A.C.H. and Kavvas M. (2008). Fully coupled dynamic analysis of a real earth dam overlaying a stiff natural clayey deposit using an advanced constitutive model. Proc. 12th Int. Conf. of IACMAG, Goa, India, 2750-2757.
- 3-4. Amorosi A., Boldini D., Elia G. (2010). Parametric study on seismic ground response by finite element modelling. Comput. Geotech., 37(4), 515-528.
- 4-5. Arulanandan K., Scott R.F. Eds. (1993). Proceedings of VELACS symposium. A.A., Balkema, Rotterdam.
- 5-6. Aydingun O., Adalier K. (2003). Numerical analysis of seismically induced liquefaction in earth embankment foundations. Part I. Benchmark model. Can. Geotech. J., 40(4), 753-765.
- 6-7. Bardet J.P. (1986). Bounding surface plasticity model for sands. J. Engng. Mech. ASCE, 112(11), 1198-1217.
8. Biot M.A. (1941). General theory of three-dimensional consolidation. J. Appl. Phys., 12, 155-164.
9. Bonilla L.F., Archuleta R.J., Lavallée D. (2005). Hysteretic and dilatant behavior of cohesionless soils and their effects on nonlinear site response: field data observations and modeling. Bull. Seism. Soc. America, 95(6), 2373-2395.
- 7-10. Borja R.I., Chao H-J., Montáns F.J., Lin C-H. (1999). Nonlinear ground response at Lotung LSST site. J. Geotech. and Geoenv. Engng. ASCE, 125(3), 187-197.
- 8-11. Calabresi G., Rampello S., Sciotti A. and Amorosi A. (2000). Diga sulla Marana Capacciotti: Verifiche delle condizioni di stabilità e analisi del comportamento in condizioni sismiche. Research Report, Università di Roma "La Sapienza".
- 9-12. Calabresi G., Rampello S., Callisto L., Cascone E. (2004). Diga S. Pietro sul fiume Osento. Verifica delle condizioni di stabilità e analisi del comportamento in condizioni sismiche. Research Report, Università di Roma "La Sapienza".

- ~~10-13.~~ Cascone E., Rampello S. (2003). Decoupled seismic analysis of an earth dam. *Soil Dyn. Earthq. Engng.*, 23(5), 349-365.
- ~~11-14.~~ Castro G., Christian J.T. (1976). Shear strength of soils and cyclic loading. *J. Geotech. Engng. ASCE*, 102(GT9), 887-894.
- ~~12-15.~~ Chan A.H.C. (1995). User Manual for DIANA-SWANDYNE II. School of Engineering, University of Birmingham, UK.
- ~~13-16.~~ Clough R.W. and Penzien J. (1993). *Dynamics of Structures* (2nd ed.). Mc. Graw-Hill, New York.
- ~~14-17.~~ Dafalias Y.F., Popov E.P. (1975). A model of nonlinearly hardening materials for complex loading. *Acta Mechanica*, 21(3), 173-192.
- ~~15-18.~~ Dakoulas P., Gazetas G. (2005). Seismic effective-stress analysis of caisson quay walls: application to Kobe. *Soils Found.*, 45(4), 133-147.
- ~~19.~~ Dakoulas P., Gazetas G. (2008). Insight into seismic earth and water pressures against caisson quay walls. *Géotechnique*, 58(2), 95-111.
- ~~16-20.~~ Delépine N., Lenti L., Bonnet G., Semblat J-F. (2009). Nonlinear viscoelastic wave propagation: an extension of Nearly Constant Attenuation models. *J. Engng. Mech. ASCE*, 135(11), 1305-1314.
- ~~17-21.~~ Dewoolkar M.M., Ko H.-Y., Pak R.Y.S. (2001). Seismic behaviour of cantilever retaining walls with liquefiable backfills. *J. Geotech. and Geoenv. Engng. ASCE*, 127(5), 424-435.
- ~~18-22.~~ Elgamal A.-W., Parra E., Yang Z., Adalier K. (2002). Numerical analysis of embankment foundation liquefaction countermeasures. *J. Earthq. Engng.*, 6(4), 447-471.
- ~~19-23.~~ Elia G. (2004). Analisi FEM di problemi al contorno in condizioni statiche e dinamiche con un modello costitutivo avanzato. Ph.D. Thesis, Technical University of Bari, Italy.
- ~~24.~~ Elia G., Amorosi A., Chan A.H.C. (2004). Nonlinear ground response: effective stress analyses and parametric studies. Japan-Europe Seismic Risk Workshop, Bristol, UK.
- ~~20-25.~~ Elia G., Amorosi A., Chan A.H.C. (2005). Fully coupled dynamic analysis of an earth dam using a complex constitutive assumption. *Proc. 11th Int. Conf. of IACMAG, Turin, Italy*, 257-264.
- ~~21-26.~~ Elia G., Amorosi A., Chan A.H.C., Kavvas M. (2010). Fully coupled dynamic analysis of an earth dam. *Géotechnique* (accepted for publication).
- ~~22-27.~~ Galadini F., Meletti C., Rebez A. Eds. (2000). *Le ricerche del GNDT nel campo della pericolosità sismica (1996-1999)*. CNR-Gruppo Nazionale per la Difesa dai Terremoti, Roma, 397 pp.

28. Gruppo di Lavoro MPS (2004). Redazione della mappa di pericolosità sismica prevista dall'Ordinanza PCM 3274 del 20 marzo 2003. Rapporto conclusivo per il Dipartimento della Protezione Civile, INGV, Milano - Roma, 65 pp.
- ~~23-29.~~ [Hancock J., Bommer J.J., Stafford P.J. \(2008\). Numbers of scaled and matched accelerograms required for inelastic dynamic analyses. *Earth. Engng. Struct. Dyn.*, 37\(14\), 1585-1607.](#)
30. Katona M.G., Zienkiewicz O.C. (1985). A unified set of single step algorithms Part 3: the Beta-m method, a generalisation of the Newmark scheme. *Int. J. Num. Meth. Engng.*, 21, 1345-1359.
- ~~24-31.~~ [Kausel E., Assimaki D. \(2002\). Seismic simulation of inelastic soils via frequency-dependent moduli and damping. *J. Engng. Mech. ASCE*, 128\(1\), 34-47.](#)
- ~~25-32.~~ Kavvadas M., Amorosi A. (2000). A constitutive model for structured soils. *Géotechnique*, 50(3), 263-273.
- ~~26-33.~~ Kwok A.O.L., Stewart J.P., Hashash Y.M.A., Matasovic N., Pyke R., Wang Z., Yang Z. (2007). Use of exact solutions of wave propagation problems to guide implementation of nonlinear seismic ground response analysis procedures. *J. Geotech. and Geoenv. Engng. ASCE*, 133(11), 1385-1398.
- ~~27-34.~~ Liu H., Song E. (2005). Seismic response of large underground structures in liquefiable soils subjected to horizontal and vertical earthquake excitations. *Comput. Geotech.*, 32(4), 223-244.
- ~~28-35.~~ Mroz Z., Norris V.A., Zienkiewicz O.C. (1978). An anisotropic hardening model for soils and its application to cyclic loading. *Int. J. Num. Anal. Meth. Geomech.*, 2, 203-221.
- ~~29-36.~~ Mucciarelli M., Gallipoli M.R. (2006). Comparison between Vs30 and other estimates of site amplification in Italy. *Proc. First European Conf. on Earth. Engng. and Seism.*, Geneva, Switzerland.
37. Muraleetharan K.K., Deshpande S., Adalier K. (2004). Dynamic deformations in sand embankments: centrifuge modelling and blind, fully coupled analyses. *Can. Geotech. J.*, 41(1), 48-69.
- ~~30-38.~~ [Newmark N.M. \(1965\). Effect of earthquake on dams and embankments. *Géotechnique*, 15\(2\), 139-160.](#)
- ~~31-39.~~ Pastor M., Zienkiewicz O.C. (1986). A generalized plasticity hierarchical model for sand under monotonic and cyclic loading. In: Pande G.N., Van Impe W.F. (Eds.), *Proc. 2nd Int. Conf. on Numerical Models in Geomechanics*, 131-150.
- ~~32-40.~~ Pastor M., Zienkiewicz O.C., Chan A.H.C. (1990). Generalized plasticity and the modelling of soil behaviour. *Int. J. Num. Anal. Meth. Geomech.*, 14, 151-190.
- ~~33-41.~~ Poulos H.G., Booker J.R., Ring G.J. (1972). Simplified calculation of embankment deformations. *Soils Found.*, 12(4), 1-17.
- ~~34-42.~~ Prevost J.H. (1978). Plasticity theory for soil stress-strain behaviour. *J. Engng. Mech. ASCE*, 104(5), 1177-1194.

35-43. Rampello S., Callisto L., Fargnoli P., Amorosi A., Elia G. (2005). Diga S. Pietro sul fiume Osento. Analisi
dinamica del comportamento della diga in presenza di sisma. Research Report, Università di Roma "La
Sapienza".

44. Sangrey D.A., Henkel D.J., Esrig M.I. (1969). The effective stress response of a saturated clay soil to repeated
loading. Can. Geotech. J., 6(3), 241-252.

45. Schnabel P.B., Lysmer J., Seed H.B. (1972). SHAKE: A computer program for earthquake response analysis of
horizontally layered sites. Report No EERC 72-12, Earthquake Engineering Research Center, University of
California, Berkeley, USA.

36-46. Semblat J-F., Gandomzadeh A., Lenti L. (2010). A simple numerical absorbing layer method in elastodynamics.
C. R. Mecanique 338(1), 24-32.

37-47. Sica S., Pagano L., Modaressi A. (2008). Influence of past loading history on the seismic response of earth dams.
Comput. Geotech., 35(1), 61-85.

38-48. Vucetic M., Dobry R. (1991). Effects of the soil plasticity on cyclic response. J. Geotech. Engng. ASCE, 117(1),
89-107.

39-49. Zienkiewicz O.C., Chan A.H.C., Pastor M., Schrefler B.A., Shiomi T. (1999). Computational Geomechanics
(with special reference to earthquake engineering). Wiley & Sons, Chichester.

~~Woodward P.K., Griffiths D.V. (1996). Influence of viscous damping in the dynamic analysis of an earth dam using
simple constitutive models. Comput. Geotech., 19, 245-263.~~

Table I: Characteristics of the input motions used in the dynamic analyses of the Marana Capacciotti dam

<i>Input</i>	T_R (years)	a_{max} - <i>outcrop</i> (g)	a_{max} - <i>bedrock</i> (g)	f_{max} (Hz)	<i>Dominant frequency</i> (Hz)	<i>Record length</i> (sec)
<i>LOMA_1</i>	1000	0.275	0.177	10	1.39	40.0
<i>LOMA_2</i>	475	0.194	0.128	10	1.39	40.0
<i>TOLMEZZO</i>	1000	0.275	0.214	10	1.49	35.0
<i>NOCERA</i>	1000	0.275	0.148	10	2.63	40.0

Table II: Characteristics of the input motions used in the dynamic analyses of the San Pietro dam

<i>Input</i>	T_R (years)	a_{max} - <i>bedrock</i> (g)	v_{max} (m/s)	T_D (s)	I_A (m/s)	f_{max} (Hz)	<i>Dominant frequency</i> (Hz)	<i>Record length</i> (sec)
Real	475	0.35	0.65	69.6	4.4	10	0.51	72.7
Artificial	475	0.41	0.38	26.4	4.1	10	4.34	30.0

Figure 1

[Click here to download Figure: Figure_01.pdf](#)

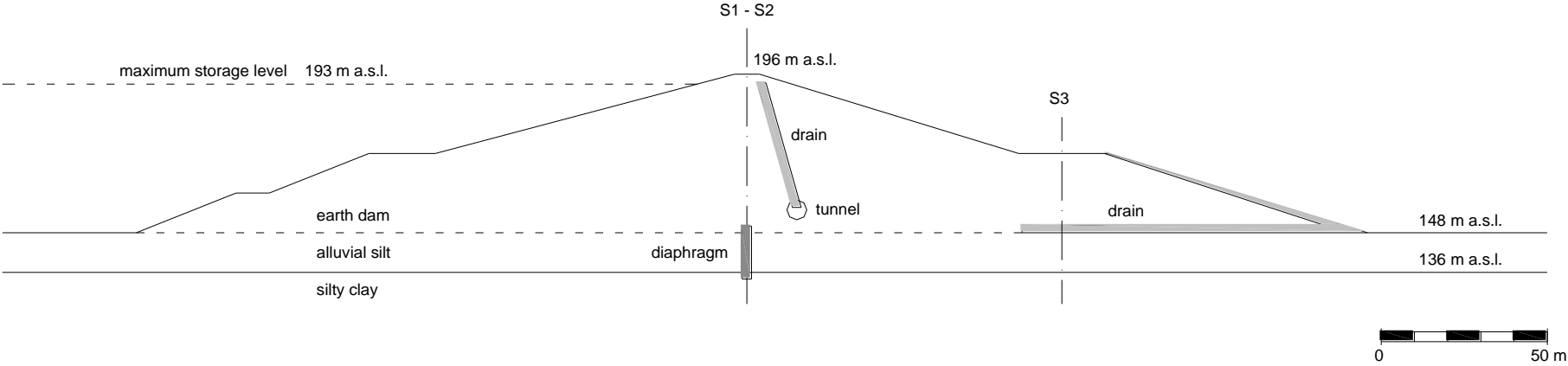


Figure 2

[Click here to download Figure: Figure_02.pdf](#)

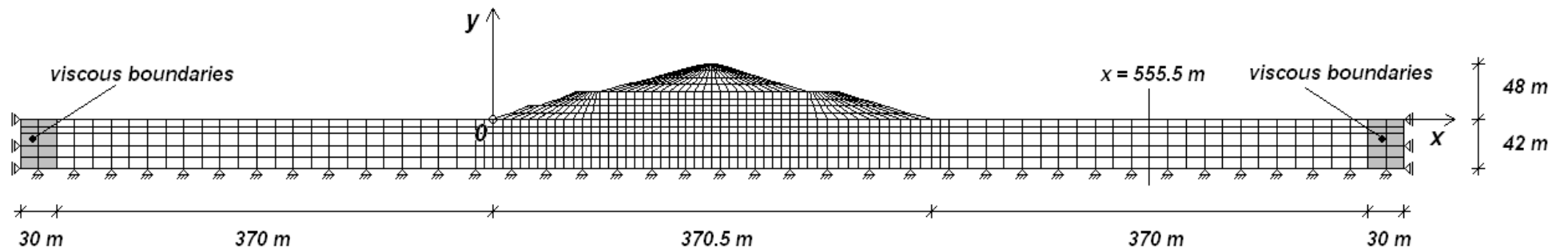


Figure 3

[Click here to download Figure: Figure_03.pdf](#)

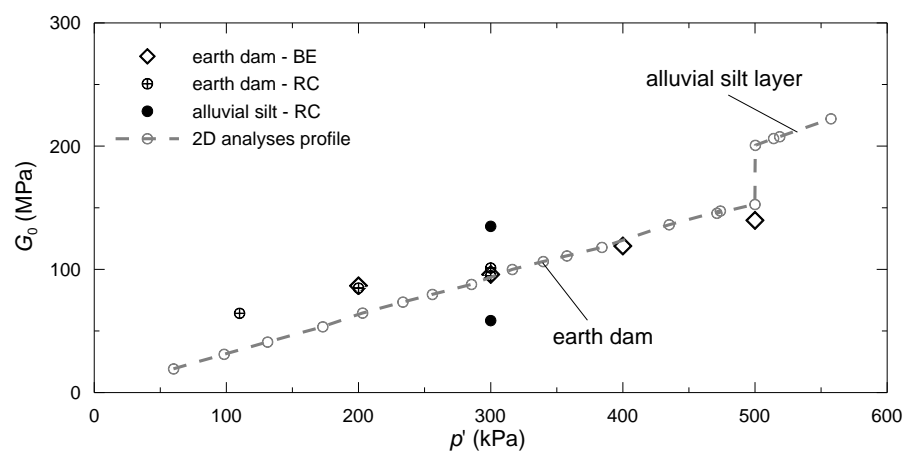


Figure 4
[Click here to download Figure: Figure_04.pdf](#)

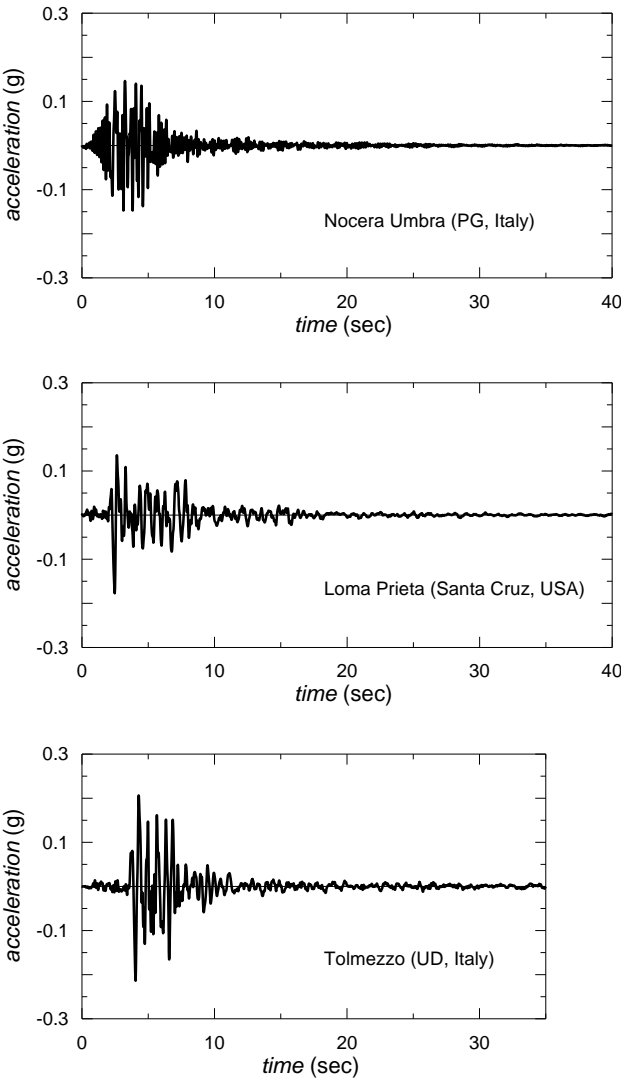


Figure 5
[Click here to download Figure: Figure_05.pdf](#)

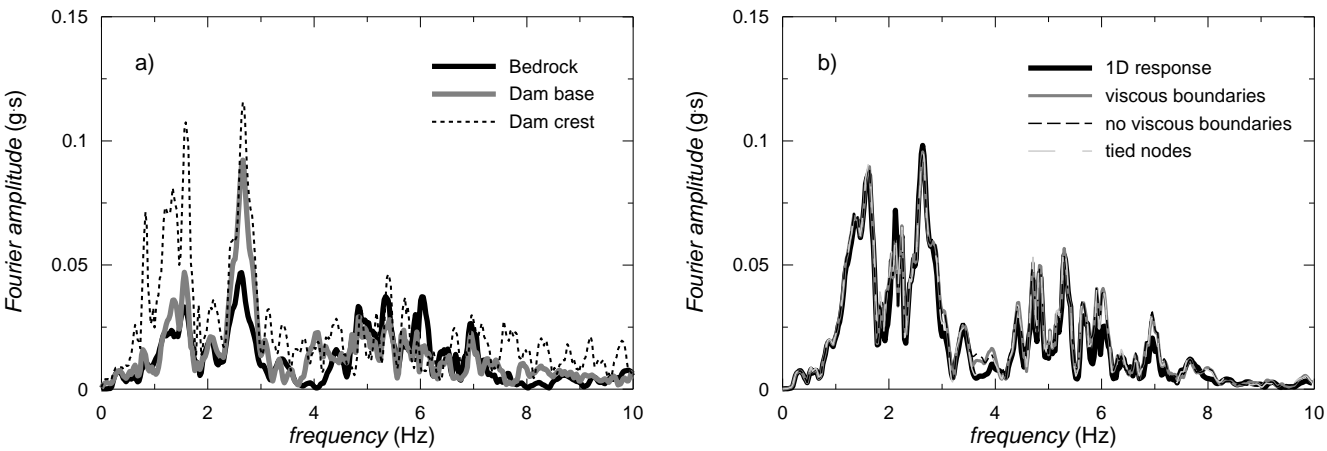


Figure 6

[Click here to download Figure: Figure_06.pdf](#)

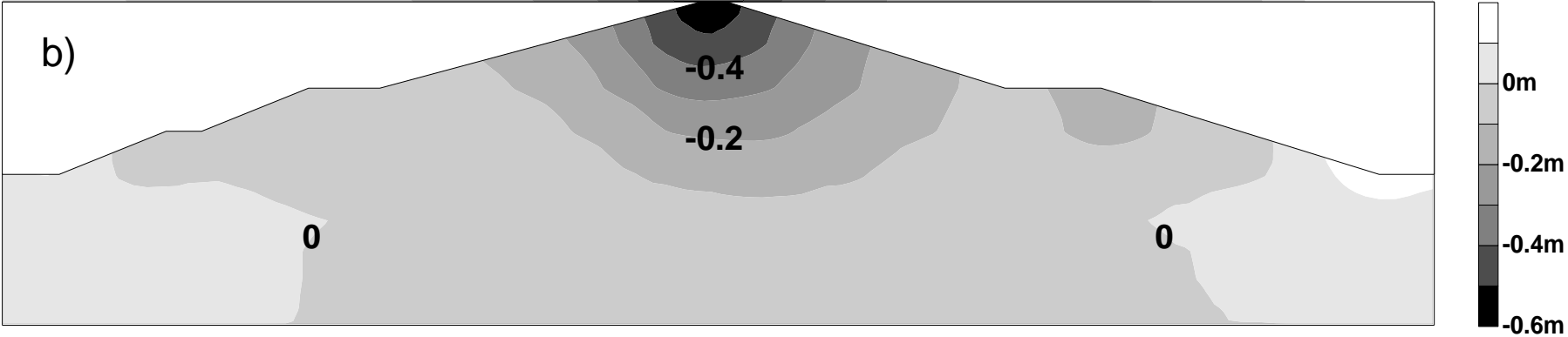
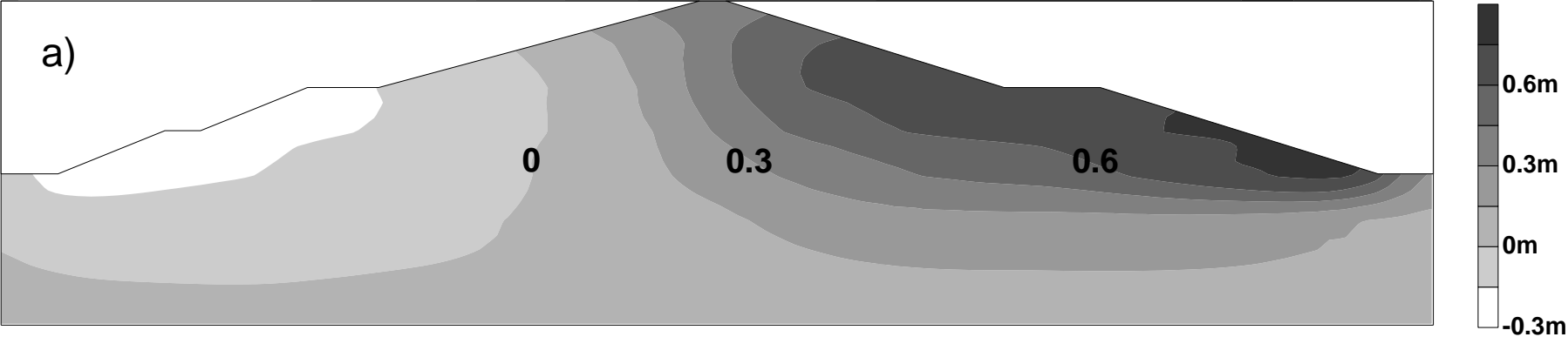


Figure 7
[Click here to download Figure: Figure_07.pdf](#)

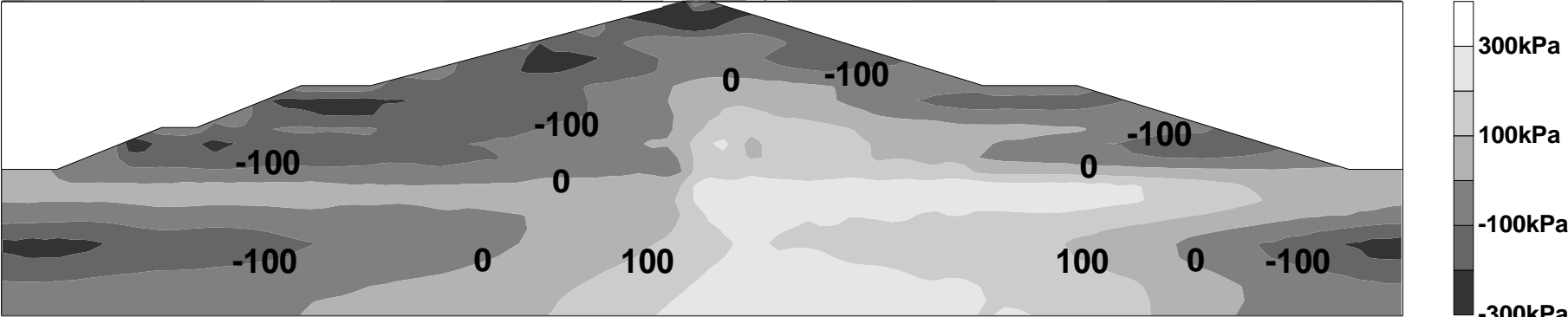


Figure 8

[Click here to download Figure: Figure_08.pdf](#)

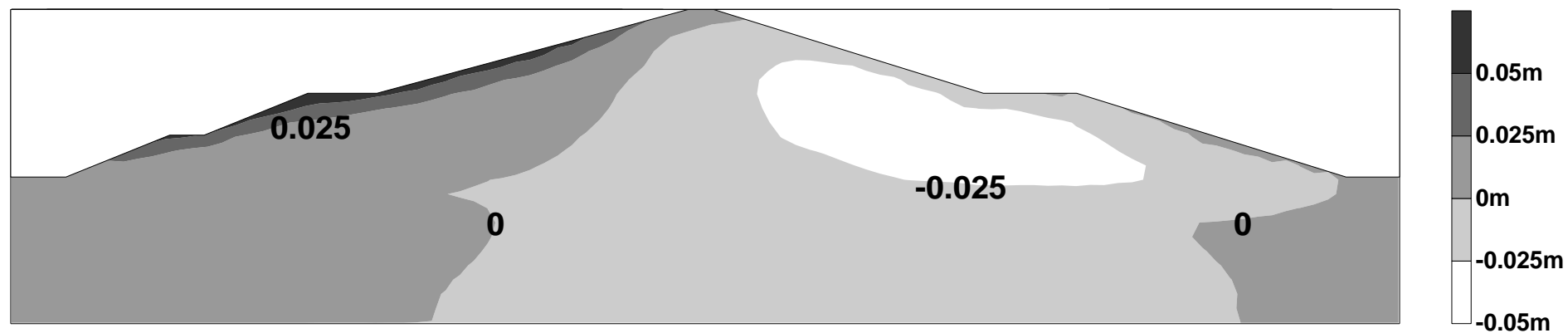


Figure 9

[Click here to download Figure: Figure_09.pdf](#)

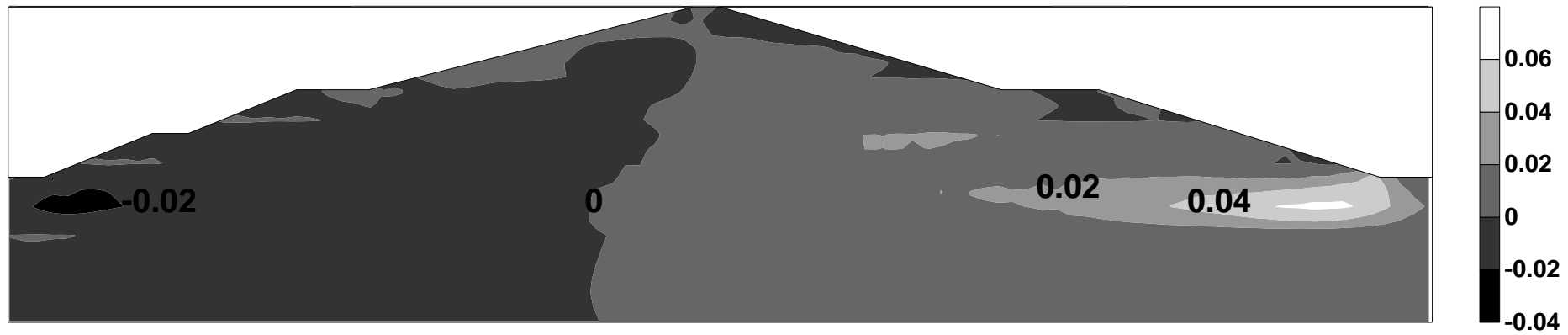


Figure 10

[Click here to download Figure: Figure_10.pdf](#)

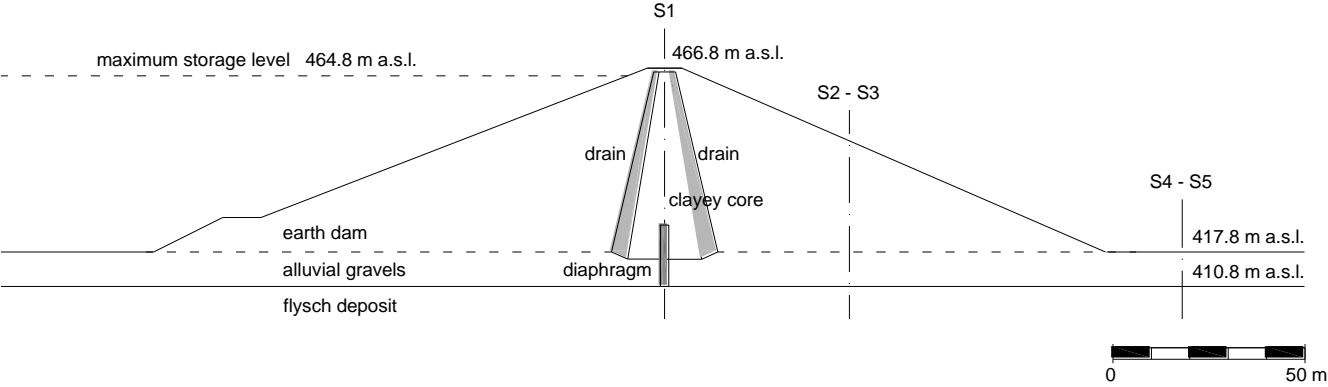


Figure 11

[Click here to download Figure: Figure_11.pdf](#)

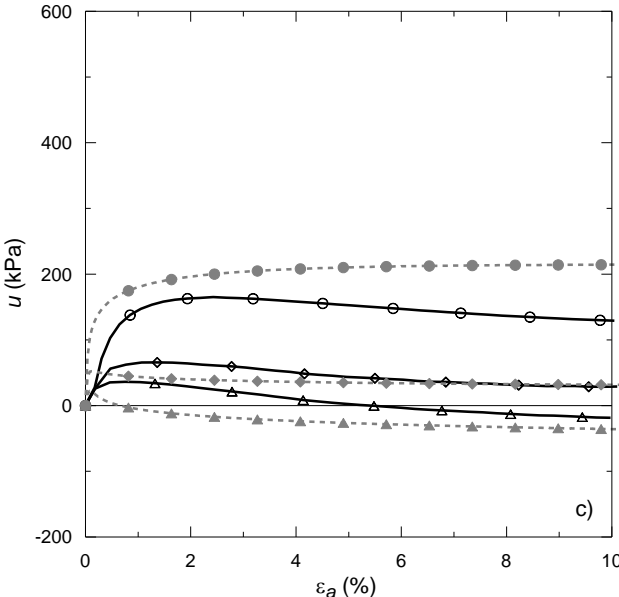
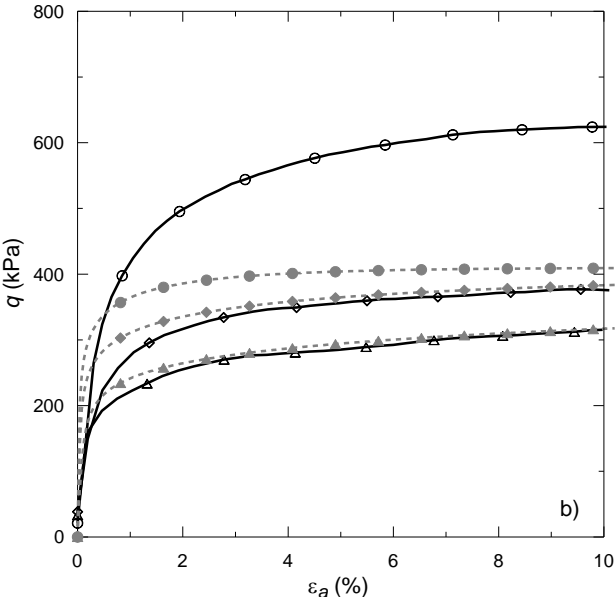
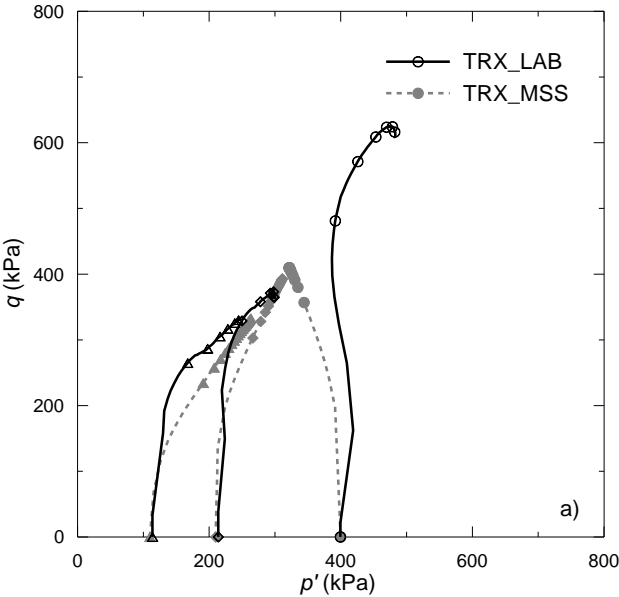


Figure 12

[Click here to download Figure: Figure_12.pdf](#)

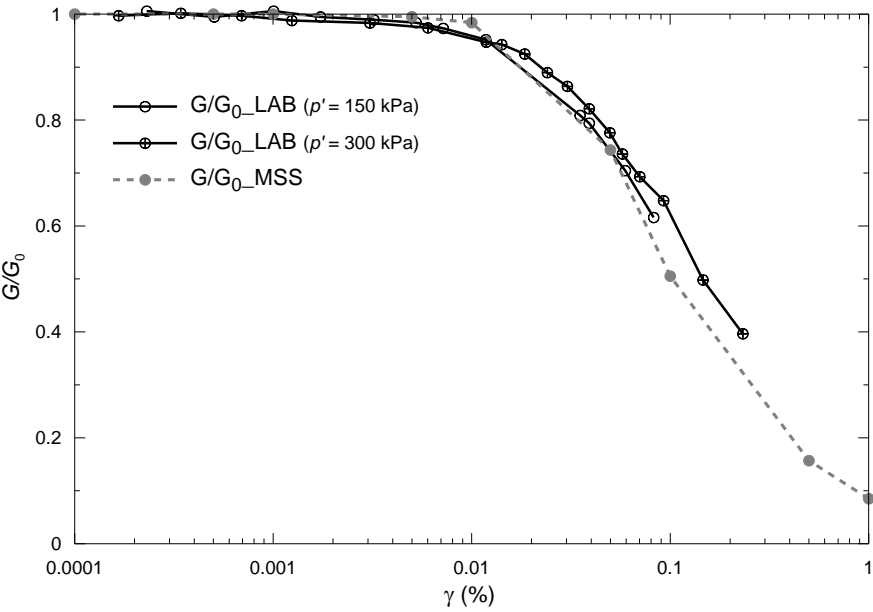


Figure 13

[Click here to download Figure: Figure_13.pdf](#)

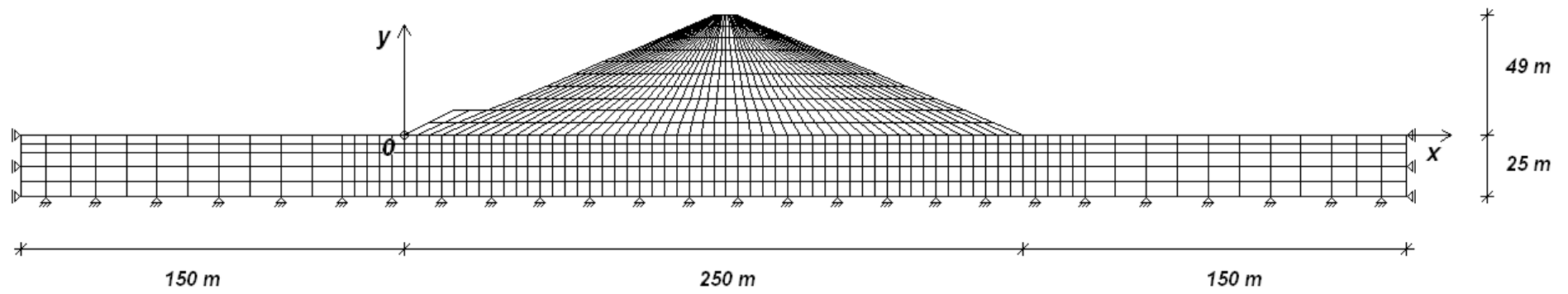


Figure 14

[Click here to download Figure: Figure_14.pdf](#)

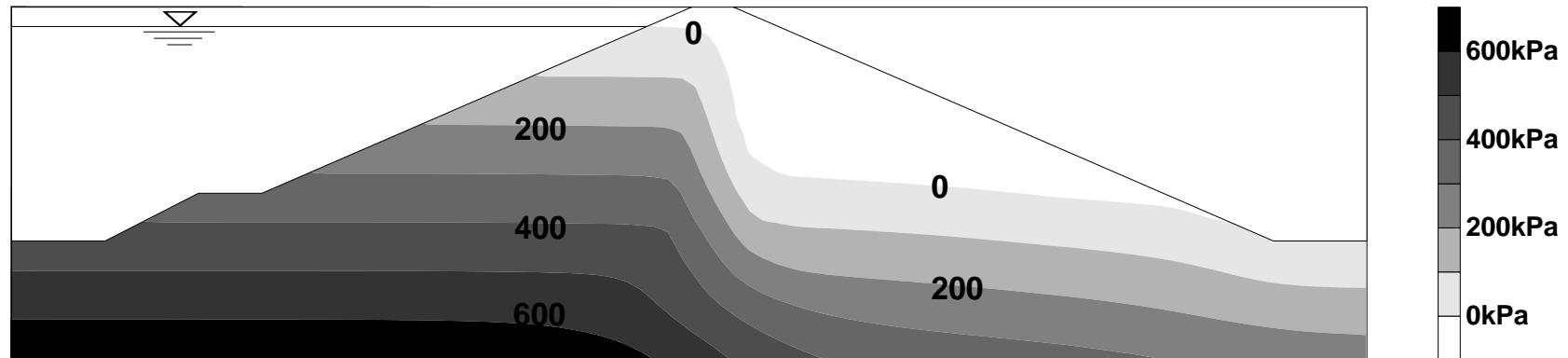


Figure 15

[Click here to download Figure: Figure_15.pdf](#)

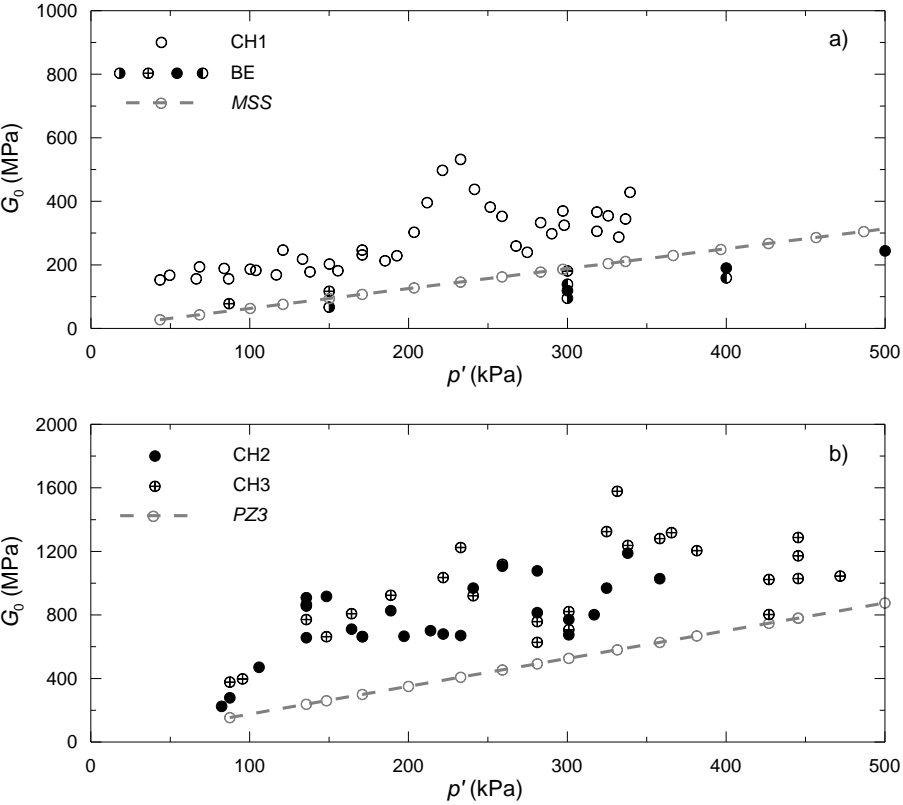


Figure 16

[Click here to download Figure: Figure_16.pdf](#)

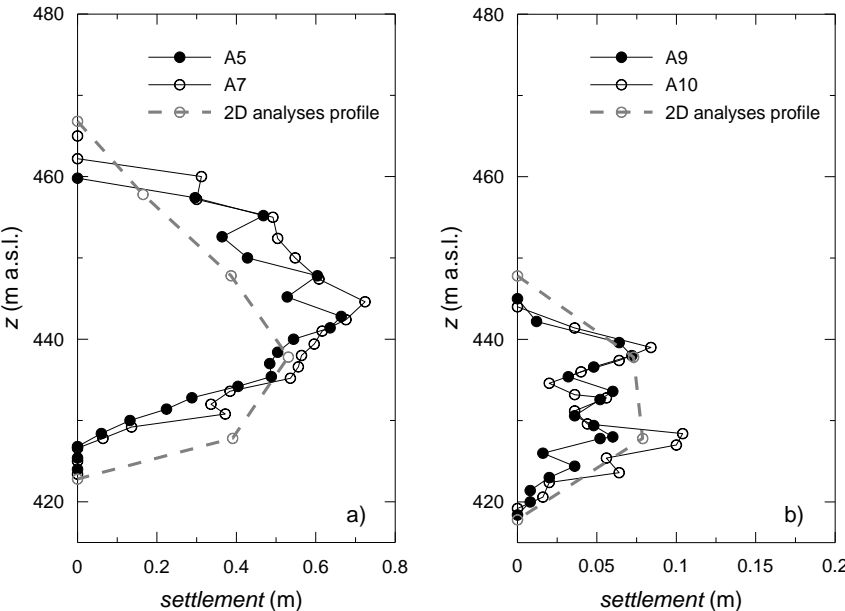


Figure 17

[Click here to download Figure: Figure_17.pdf](#)

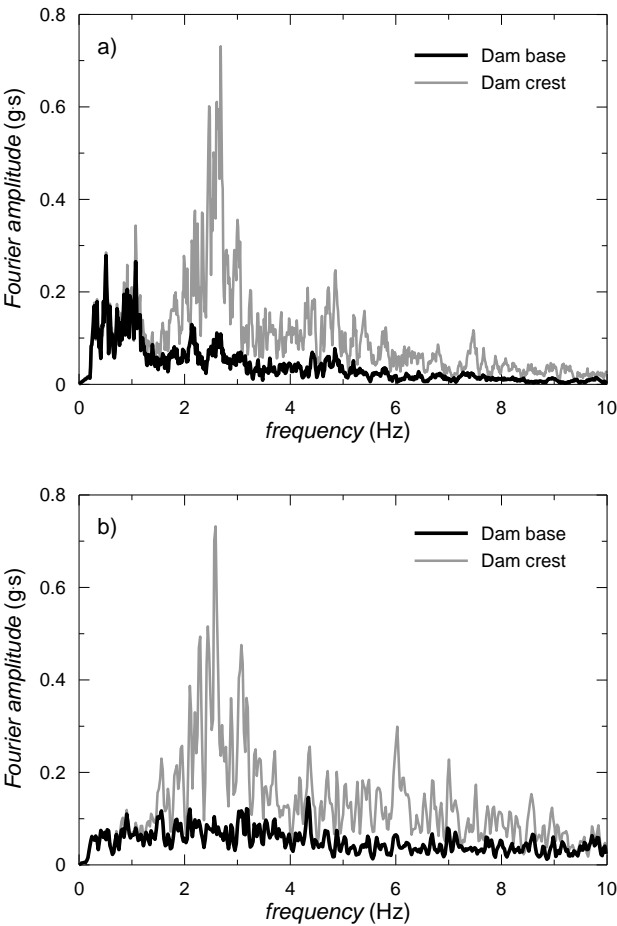


Figure 18

[Click here to download Figure: Figure_18.pdf](#)

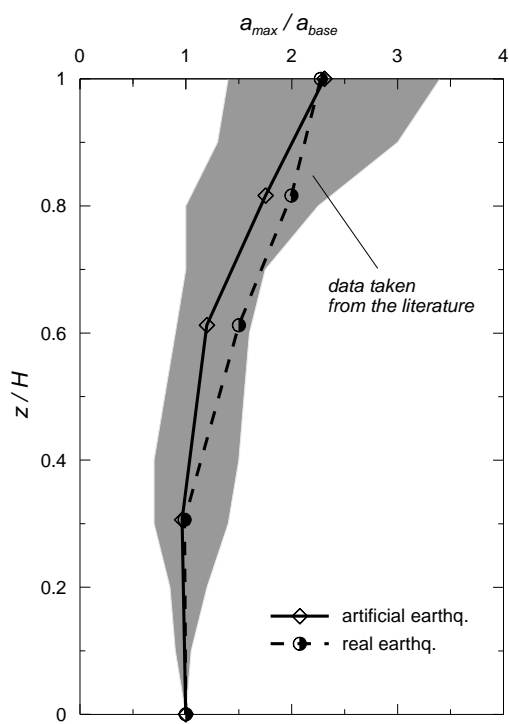


Figure 19

[Click here to download Figure: Figure_19.pdf](#)

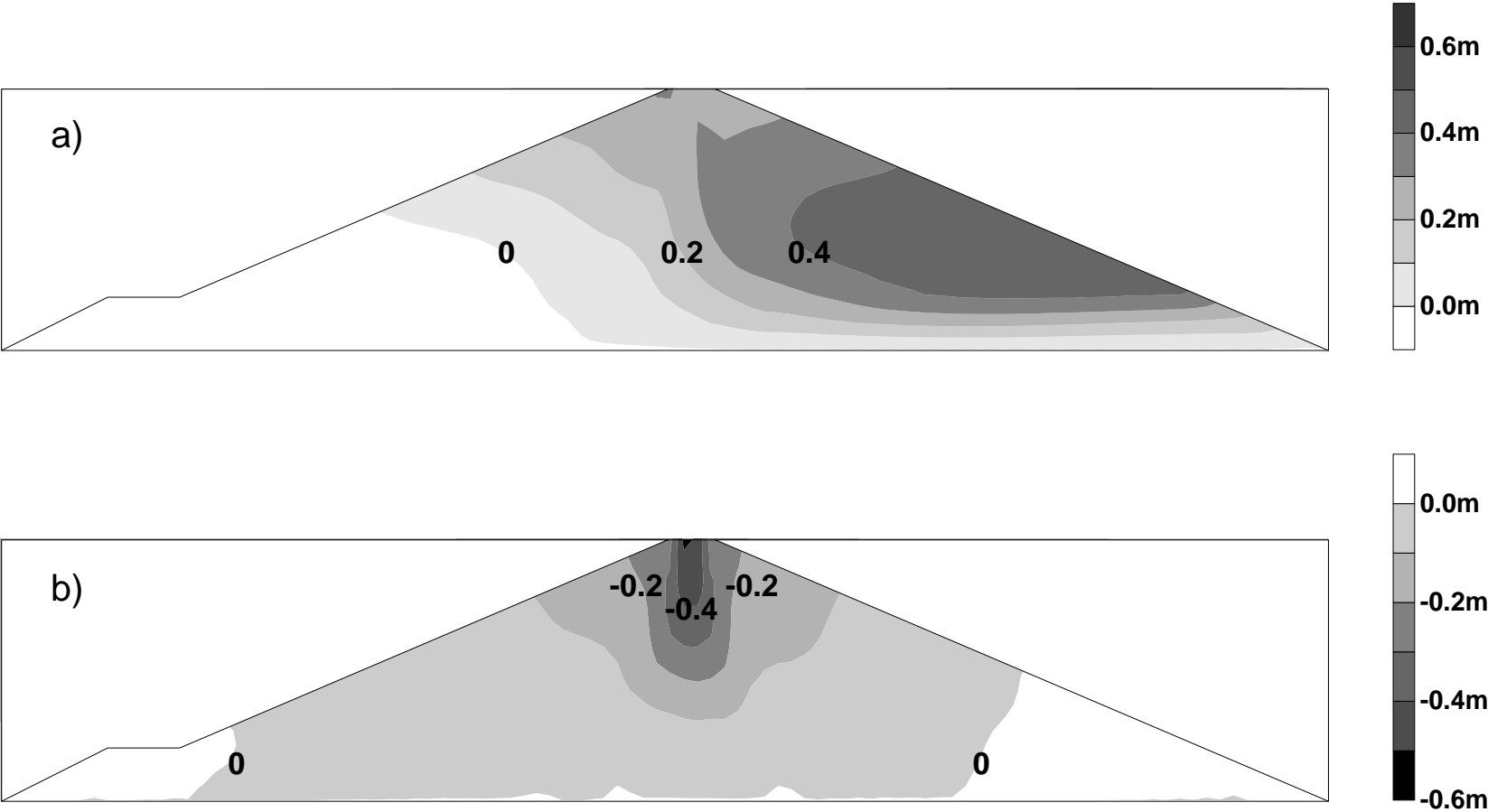


Figure 20

[Click here to download Figure: Figure_20.pdf](#)

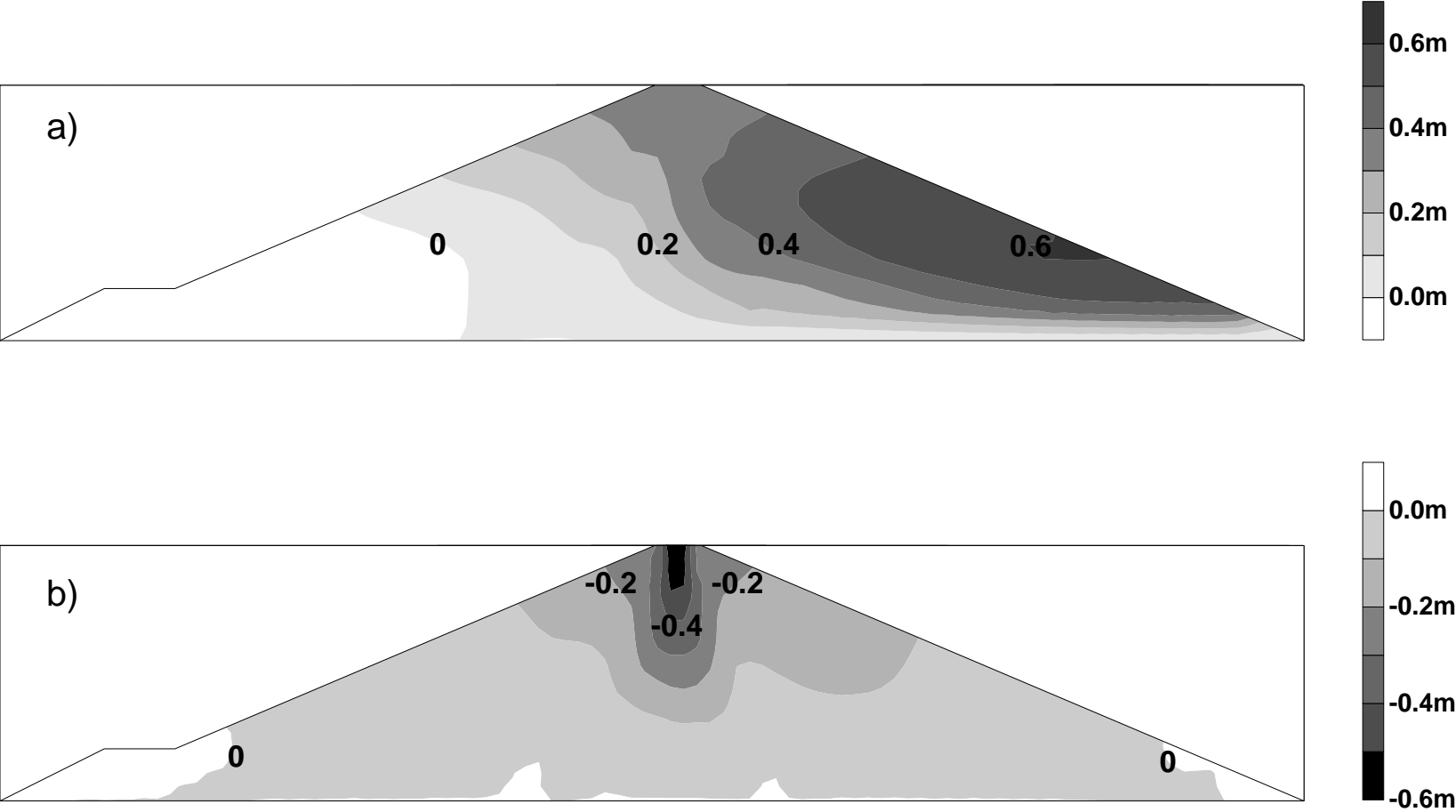


Figure 21

[Click here to download Figure: Figure_21.pdf](#)

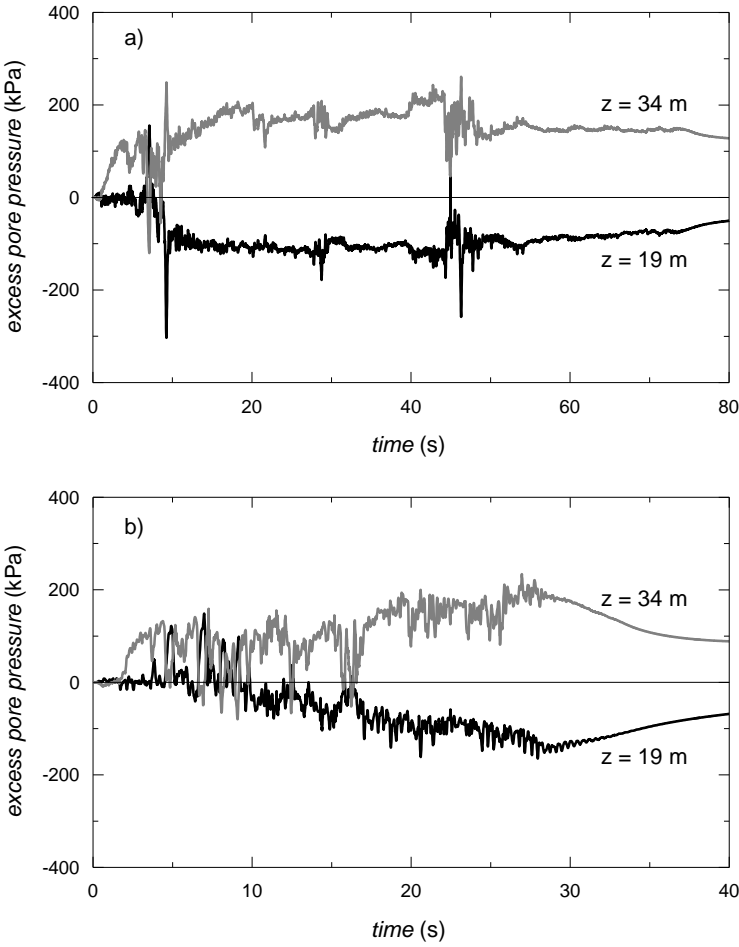


Figure 22

[Click here to download Figure: Figure_22.pdf](#)

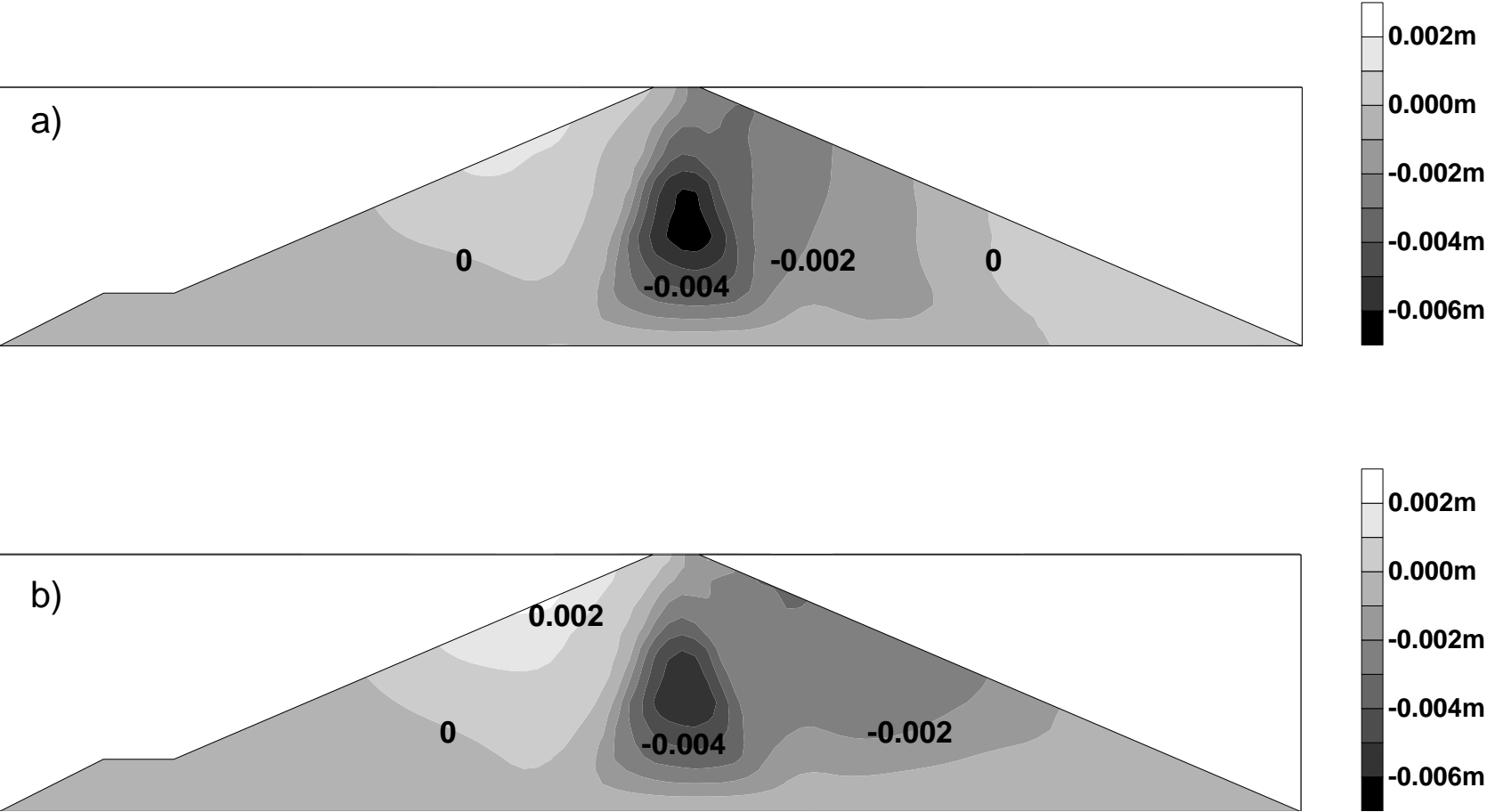


Figure 23

[Click here to download Figure: Figure_23.pdf](#)

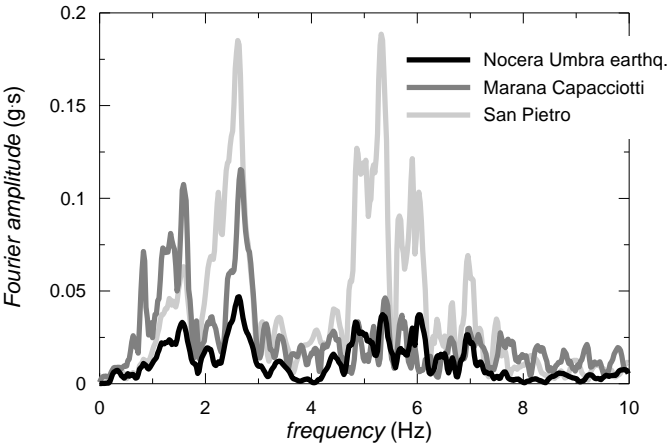
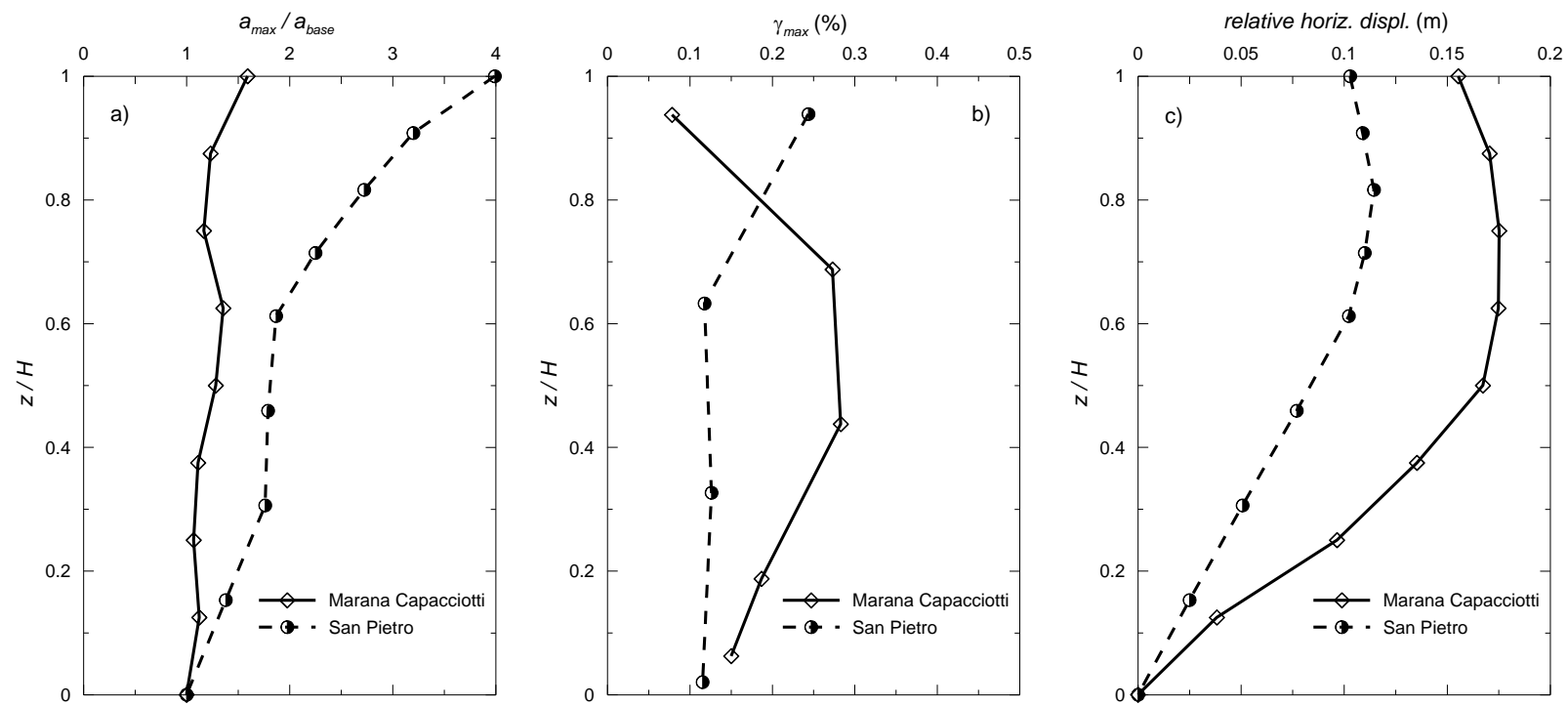


Figure 24

[Click here to download Figure: Figure_24.pdf](#)



List of figure captions

Figure 1. Cross-section of the Marana Capacciotti dam.

Figure 2. FE mesh and boundary conditions adopted for the Marana Capacciotti dam.

Figure 3. Comparison between the results of resonant column and bender element tests and the initial shear modulus profile computed along the dam axis at the end of the static analyses of the Marana Capacciotti dam.

Figure 4. Acceleration time histories of the input motions employed in simulations of the Marana Capacciotti dam.

Figure 5. Comparison between the Fourier spectra computed: a) along the Marana Capacciotti dam axis and b) at ground level along the vertical $x = 555.5$ m assuming different boundary conditions.

Figure 6. Contour lines of: a) horizontal and b) vertical displacements at the end of the shaking (Marana Capacciotti dam).

Figure 7. Contour lines of excess pore pressures at the end of the shaking (Marana Capacciotti dam).

Figure 8. Contour lines of additional settlements due to consolidation (Marana Capacciotti dam).

Figure 9. Contour lines of shear strains at the end of the shaking (Marana Capacciotti dam).

Figure 10. Cross-section of the San Pietro dam.

Figure 11. Comparison between experimental results of undrained triaxial compression tests performed on the silty clay soil of the San Pietro dam core and the computed response with *MSS*: a) stress paths; b) deviatoric stress - axial strain curves and c) pore pressures - axial strain curves.

Figure 12. Comparison between experimental results of resonant column tests performed on the silty clay soil of the San Pietro dam core and the computed response with *MSS*.

Figure 13. FE mesh and boundary conditions adopted for the San Pietro dam.

Figure 14. Contour lines of pore water pressures at the end of the seepage analysis (San Pietro dam).

Figure 15. Comparison between the laboratory data and the computed G_0 profiles relative to: a) the core and b) the shells of the San Pietro dam.

Figure 16. Comparison between the observed settlements and the FE analysis profiles obtained along: a) the core and b) the shells of the San Pietro dam.

Figure 17. Comparison between the Fourier spectra obtained along the San Pietro dam axis applying at the bedrock level: a) the real and b) the artificial input motion.

Figure 18. a_{max}/a_{base} profiles computed at the end of the FE dynamic analyses of the San Pietro dam and comparison with literature results.

Figure 19. Contour lines of: a) horizontal and b) vertical displacements obtained using the real input motion (San Pietro dam).

Figure 20. Contour lines of: a) horizontal and b) vertical displacements obtained using the artificial input motion (San Pietro dam).

Figure 21. Excess pore water pressure time histories along the San Pietro dam axis computed applying: a) the real and b) the artificial input motion.

Figure 22. Contour lines of consolidation settlements relative to: a) the real and b) the artificial input motion analysis (San Pietro dam).

Figure 23. Comparison in terms of Fourier spectra recorded at crest between the Marana Capacciotti and the San Pietro dam analyses performed applying the same input motion at bedrock.

Figure 24. Comparison between the Marana Capacciotti and the San Pietro dam analyses in terms of: a) profiles of a_{max}/a_{base} along the dam axes, b) profiles of maximum shear strain with depth and c) profiles of maximum horizontal displacement relative to the dam base with depth.

AMERICAN SOCIETY OF CIVIL ENGINEERS
COPYRIGHT TRANSFER AGREEMENT

Publication Title: INTERNATIONAL JOURNAL OF GEOMECHANICS
Manuscript/Chapter Title: NUMERICAL PREDICTION OF THE DYNAMIC BEHAVIOUR
OF TWO EARTH DAMS IN ITALY USING A FULLY-COUPLED
NON-LINEAR APPROACH

Author(s) - Names and addresses of all authors

GAETANO ELIA - NEWCASTLE UNIV. - NE1 7RU NEWCASTLE UPON TYNE, UK

ANGELO AMOROSI - TECHNICAL UNIV. OF BARI - VIA ORABONA 4, 70125 BARI, ITALY

ANDREW CHAN - UNIV. OF BIRMINGHAM - B15 2TT BIRMINGHAM, UK

MICHAEL KAVVADAS - NATIONAL TECHNICAL UNIV. ATHENS - ZOGRAFOU 157 80

The author(s) warrants that the above-cited manuscript is the original work of the author(s) and has never been published in its present form.

ATHENS, GREECE

The undersigned, with the consent of all authors, hereby transfers, to the extent that there is copyright to be transferred, the exclusive copyright interest in the above-cited manuscript (subsequently called the "work") in this and all subsequent editions of the work, and in derivatives, translations, or ancillaries, in English and in foreign translations, in all formats and media of expression now known or later developed, including electronic, to the American Society of Civil Engineers subject to the following.

- The undersigned author and all coauthors retain the right to revise, adapt, prepare derivative works, present orally, or distribute the work provided that all such use is for the personal noncommercial benefit of the author(s) and is consistent with any prior contractual agreement between the undersigned and/or coauthors and their employer(s).
- In all instances where the work is prepared as a "work made for hire" for an employer, the employer(s) of the author(s) retain(s) the right to revise, adapt, prepare derivative works, publish, reprint, reproduce, and distribute the work provided that such use is for the promotion of its business enterprise and does not imply the endorsement of ASCE.
- No proprietary right other than copyright is claimed by ASCE.
- An author who is a U.S. Government employee and prepared the above-cited work does not own copyright in it. If at least one of the authors is not in this category, that author should sign below. If all the authors are in this category, check this box ☐ and sign here: _____. Please return this form by mail.

SIGN HERE FOR COPYRIGHT TRANSFER [Individual Author or Employer's Authorized Agent (work made for hire)]

GAETANO ELIA

Print Author's Name

Print Agent's Name & Title

Gaetano Elia

Signature of Author (in ink)

Signature of Agency Rep (in ink)

Date: 13/06/2010

Note: If the manuscript is not accepted by ASCE or is withdrawn prior to acceptance by ASCE, this transfer will be null and void.

Ref.: Ms. No. GMENG-85

Numerical prediction of the dynamic behaviour of two earth dams in Italy using a fully-coupled non-linear approach GAETANO ELIA, Ph.D.; ANGELO AMOROSI, Ph.D.; ANDREW H.C. CHAN, Ph.D.; MICHAEL J. KAVVADAS, Ph.D.

Dear Dr. ELIA,

Your Technical Paper, listed above, has completed a review for publication in ASCE's International Journal of Geomechanics. The editor has requested that minor revisions be made based on the reviewers' evaluations (shown at the end of this email) and submitted for by 05-21-2010. This revision will only be seen again by the editor and will not undergo the entire review process.

Please submit the revised manuscript and a detailed response to the reviewers' criticisms by logging onto the editorial management system at <http://jrngmeng.edmgr.com/>.

Be advised that the editor may request further revision or decline your revised version if all of the reviewers' comments have not been adequately addressed.

A reminder of the ASCE policy on materials sharing and data availability: if you have not fully explained your restrictions to this policy in your cover letter, please include this with your revision. To view the full policy, please contact ASCE, we will send it to you.

In addition, a reminder that you opted-in to have your paper published as a raw, uncopyedited, unformatted manuscript. This will occur within a 72-hour period of acceptance. If you do not wish to have your manuscript published at this time, please alert us immediately. You can read the full policy here: <http://pubs.asce.org/journals/pap/>

Comments from the Editor and Reviewers can be found below.

We look forward to receiving your revised manuscript.

Sincerely,

Emily Sirotta
Editorial Coordinator

Reviewers' comments:

We have received two reviews of this manuscript (see below). The comments are informative and useful. It is suggested that the manuscript be revised in light of these comments. Changes made should be highlighted in color. An itemized response to the review comments should be included at the end. Related papers published previously in IJOG should be cited. The revised manuscript will be reviewed by the editor only.

Reviewer #1: The goal of the paper is very interesting (dynamic behavior of earth dams using a fully-coupled nonlinear approach) but the paper should be revised since several important issues are unclear or not correct as presented. First of all, the main problem are the boundary conditions at the bottom of the FEM models ("by applying the real input motions to the fixed solid nodes"): it is not possible to have "fixed" nodes and to prescribe a non-zero motion (acceleration or displacement??) at the same time. The paper by Kwok et al. (2007) concerns the type of motion to consider (outcrop, in-depth, etc) but the consequence of this paper is the assumption in terms of velocity contrast (rigid or elastic bedrock) and not a choice between free or fixed boundary conditions.

As the reviewer correctly points out, the earthquake is applied as a prescribed horizontal displacement time history to the nodes at the bottom of the mesh, as it is usually modelled in many FE dynamic codes. During the dynamic simulations the nodes at the bottom of the mesh are no more fixed in both the directions, but only in the vertical one. The statement has been clarified in the paper.

In the proposed FEM models, the depths of stiff soil under the dams are small since a rigid bedrock condition should probably be deeper. Furthermore the wavefield radiated from the dam is probably strong.

In the case of the Marana Capacciotti dam, no direct seismic site measurements are available to characterise the shear stiffness profile with depth of the deep silty clay layer. Nevertheless, the depth of the rigid bedrock has been assumed on the base of typical shear wave velocity profiles measured in-situ in similar sites reported in the literature. In the case of the San Pietro dam, the cross-hole measurements allow to clearly identify the bedrock at a depth of 25m below the base of the dam. In both cases, the assumed depth of the bedrock formation has been related to the real in-situ conditions and seems reasonable.

Concerning the lateral boundary conditions, the use of two finite elements as absorbing layers is probably not sufficient. Recent results on such simple and original absorbing layer methods should be considered in the analysis (A simple numerical absorbing layer method in elastodynamics, *Comptes Rendus Mecanique*, 338(1), 2010, pp.24-32) in order to optimize the absorbing layer size, the damping values and the overall efficiency.

The lateral boundary conditions adopted in this work during the dynamic simulations of the Marana Capacciotti dam are exactly the same of those recently proposed by Semblat et al. 2010 (this reference has been added in the revised manuscript). The validation of the boundary conditions, reported in the new Fig. 5(b) and commented in section 3.3, shows that the adopted length

of the mesh is sufficient to avoid wave reflections along the vertical boundaries during the seismic action, thus indicating that the adopted boundary conditions have a negligible effect on the results of the presented FE dynamic simulation. Nevertheless, the authors agree with the reviewer that the absorbing layer size, the damping values and the overall efficiency of the method should be investigated and this will be part of future research.

These remarks only concern the motion of the solid phase; what about the boundary conditions for the fluid phase?

The u-p formulation adopted in the finite element code Swandyné II to describe the solid-fluid interaction scheme requires the solution of a system of two ordinary differential equations (once the spatial discretisation has been performed): one for the solid and one for the fluid phase. While the equation relative to the solid phase gives two roots, the one relative to the fluid phase is characterized by one root only. This mathematically means that no wave is propagating in the fluid phase during the dynamic action and, therefore, no particular boundary conditions are needed for this phase. In the presented dynamic simulations, in fact, standard impermeable boundaries have been employed for the fluid phase along the vertical and bottom sides of the mesh.

Finally, the accelerograms being scaled, it should be mentioned that the scaling between different quakes must fulfil such scaling relations as those proposed by D. Boore (plot the accelerograms in order to illustrate their time variations).

The need of appropriate techniques to select, scale and match real records has been mentioned in the paper, although it is beyond the purpose of the work. As requested, a new Fig. 4 showing the acceleration time histories of the input motions employed for the dynamic analyses of the Marana Capacciotti dam has been added in the revised manuscript.

Secondly, the paper presents the seismic response of two different dams. The goal may be to compare their seismic response and stability but no direct comparison is performed. Another possibility is to consider one dam only and to discuss the results in deeper details.

As correctly suggested by the reviewer, a direct comparison between the seismic response of the two dams subjected to the same input motion has been introduced in the revised manuscript and reported in a new section 5. In order to fulfil the limits imposed on the length of the manuscript, the discussion regarding the influence of viscous damping on the results of the Marana Capacciotti analysis has been removed from the final section of the paper. The reader is referred to the work of Elia et al. (2010) for more details on the Rayleigh damping calibration. The conclusions have been included in a separate final section (new section 6).

Furthermore it is unclear how the drains, the injections and the concrete diaphragm are accounted for in the FEM model of the San Pietro dam.

Those aspects have been clarified in section 4.2.

Thirdly, in the FEM model, the wavelength/element size ratio should be estimated in order to assess the numerical accuracy for such strongly nonlinear models. In the linear range, considering a 800m/s shear wave

velocity, the wavelength is only 80m at 10Hz. What about soft soils at large shear strain (i.e. accounting for a large shear modulus decrease leading to much shorter wavelengths)?

For the soft soils involved in the two dams the average value of shear wave velocity is 250m/s. Therefore, the wavelength is 25m at 10Hz. The maximum height of the elements of the two dams is smaller than 1/4 of this minimum wavelength (25m) associated with the highest frequency component of the input wave (10Hz).

In 3.3, the (conditional) stability criterion should be given and the related frequency range estimated.

The adopted time integration scheme is unconditionally stable if the coefficients $\beta_1 \geq 0.5$, $\beta_2 \geq 0.5(0.5 + \beta_1)^2$ and $\beta_1^* \geq 0.5$ are chosen. This is the case for all the presented dynamic simulations.

Finally, here are some more specific remarks on the text and figures:

* in the introduction, seismic ground motion assessment and site effects should be mentioned and several related approaches for strong motion estimation should be recalled (incl. some references):

- equivalent linear approaches: e.g. Schnabel P.B., Lysmer J., Seed H.B. (1972). SHAKE: A computer program for earthquake response analysis of horizontally-layered sites, Report No. EERC-72/12, Earthquake Engineering Research Center, University of California at Berkeley, Berkeley, CA, USA.

- extended linear approaches : 1/ Kausel E., Assimaki D. (2002). Seismic simulation of inelastic soils via frequency-dependent moduli and damping, Journal of Engineering Mechanics (ASCE), 128(1), 34-47; 2/ Delepine N., Bonnet G., Lenti L., Semblat J-F (2009). Nonlinear viscoelastic wave propagation: an extension of Nearly Constant Attenuation models, Journal of Engineering Mechanics (ASCE), 135(11), pp.1305-1314.

- hysteretic models: 1/ Bonilla L.F., Archuleta R.J., Lavallee D. (2005). Hysteretic and Dilatant Behavior of Cohesionless Soils and Their Effects on Nonlinear Site Response: Field Data Observations and Modeling, Bulletin of the Seismological Society of America, 95(6) pp.2373-2395; 2/ Cacciola P., Biondi G., Cascone E. (2009). Site Response Analysis using the Preisach Formalism, Proc. of the 12th Int. Conf. on Civil, Structural and Environmental Eng. Computing, B.H.V. Topping, L.F. Costa Neves and R.C. Barros, (Editors), Civil-Comp Press, Stirlingshire, Scotland.

- mechanics of porous media: Coussy, O. Poromechanics, John Wiley & Sons (2004)

Seismic ground motion assessment and site effects have been mentioned in the introduction. Most of the suggested references have been recalled in the text and added in the reference section.

* the variational formulation should be briefly described (solid phase, fluid phase, etc)

The authors agree with the reviewer that the variational formulation should be recalled in the text, but this would lengthen the paper. Therefore, these details have not been reported in the manuscript and the reader is referred to the original work of Biot (1941) and Zienkiewicz et al. (1999).

* the time integration scheme should be briefly recalled (as well as the related stability conditions)

As before, the integration scheme has not been reported in the paper for the imposed limits to its length. The reader is referred to the work of Zienkiewicz et al. (1999).

* the damping variations for the Rayleigh formulation should be given earlier (esp. frequency range)

The Rayleigh formulation can be found in any standard structural dynamics textbook (e.g. Clough and Penzien, 1993) and therefore is not presented in section 2 relative to the FE code and the adopted constitutive models. As regards the frequency range used for the calibration of Rayleigh damping parameters, it looks better to introduce the relevant information in section 3.3 for the Marana Capacciotti dam and section 4.3 for the San Pietro dam, as the frequency range adopted is different for the two dams. In any case, the range employed in the dynamic simulations of the San Pietro dam has been now specified in section 4.3.

* a few equations or schematics are needed to briefly describe the mechanical models considered in the paper

Once again, the paper would become very long if such information is added. Therefore, the reader is suggested to refer to the original papers by Kavvadas & Amorosi (2000) and by Pastor et al. (1990) for the details of the constitutive models formulation.

* in section 3, the use of unit "Mm³" is probably inappropriate (does it mean 10¹⁸ m³?)

The unit "Mm³" means 10⁶ m³. The text has been changed accordingly.

* in subsect. 3.3, PGD or PGV isovalue plots may be given

In section 3.3 relative to the Marana Capacciotti dam, the old Fig. 5 showing the time histories of vertical and (relative) horizontal displacements recorded at different depths along the dam axis has been substituted with a new figure (Fig. 6) reporting the contour lines of horizontal and vertical displacements obtained at the end of the earthquake. This is also consistent with similar figures reported for the San Pietro dam.

* in most of the Figures, the text and lines are too small/thin

The figures have been revised and enlarged.

* Fig.16: is it possible to compare linear effects and nonlinear ones (i.e. geometry vs rheology)?

The authors agree with the reviewer that the comparison reported in Fig. 16 in terms of Fourier spectra recorded at dam base and dam crest includes the amplification effects due to both the 2D geometry of the embankment and the soil nonlinear mechanical behaviour, but in reality the two effects occurs together and cannot be distinguished unless a linear elastic analysis of the dam is performed.

* p.18-L.57: "obvious" instead of "evident"

The word "evident" has been changed with "clear".

* p.19: give and discuss profiles of maximum shear strain vs depth

As a direct comparison between the two dams is now included in the revised version of the manuscript (see the answer to one of the previous points raised by the reviewer), the profiles of maximum shear strain with depth are given for the new simulations presented and discussed in the final part of the paper (new section 5).

* in sect.5, the discussion on the absorbing conditions should be given earlier in the paper. The validation of these conditions should be made with the dam included since no lateral reflections should occur in a purely horizontal profile.

The discussion on the absorbing conditions has been anticipated in the text from section 5 to section 3.3. As regards the validation of the adopted boundary conditions, the new Fig. 5(b) shows the comparison in terms of Fourier spectra between different hypotheses which, in fact, include the dam on top of the foundation layer.

Reviewer #2: Seismic stability of two dams in Italy have been analysed using coupled (Biot-type) effective stress formulation. An existing elastoplastic constitutive model with multi- yield surfaces has been implemented in a finite element nonlinear code. The results included predictions with comparisons with observed results. The paper is recommended for publication after revision as per review comments.

The figures appear too small and difficult to read. They should be revised.

The figures have been revised and enlarged.